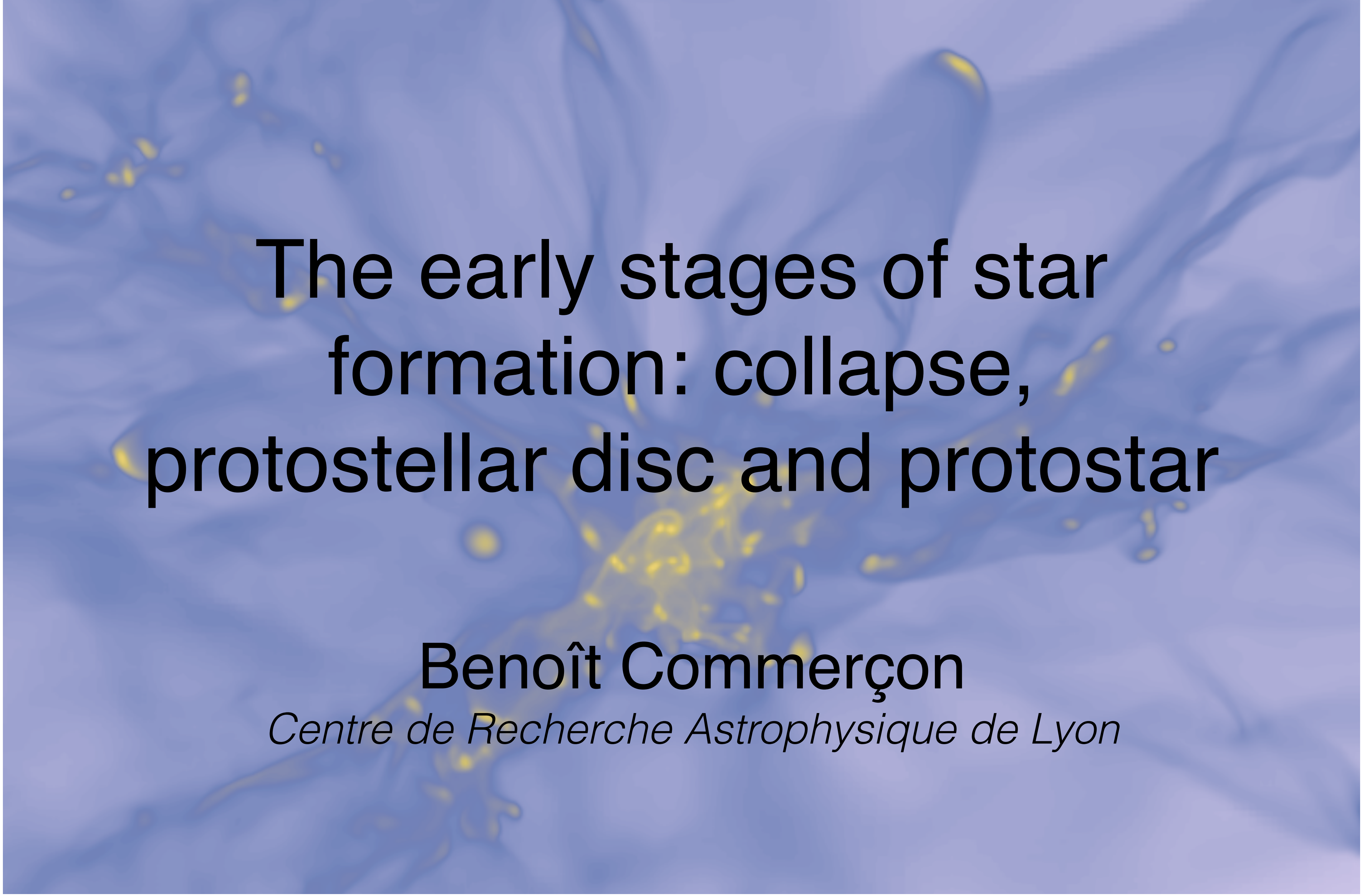

The early stages of star formation: collapse, protostellar disc and protostar

Benoît Commerçon

Centre de Recherche Astrophysique de Lyon

CENTRE DE RECHERCHE ASTROPHYSIQUE DE LYON

Outline

1. Introduction
2. Dense core collapse, disc formation (pc to au)
3. Formation of the protostar (au to $R_\odot$)
4. Observations
5. Perspectives

Interstellar matter cycle

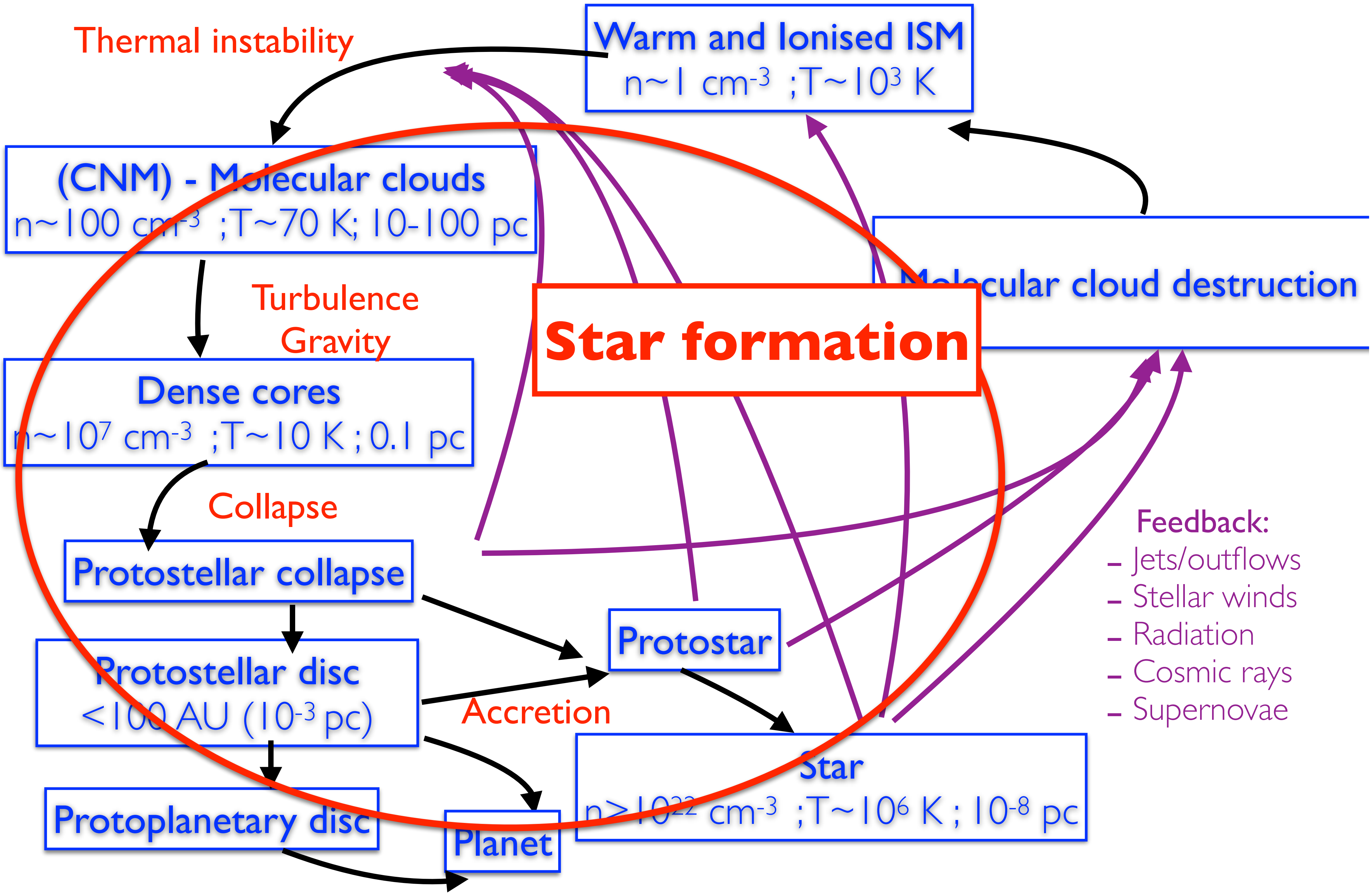

What do we find in the interstellar medium?

- photons at all wavelengths
- gas (mainly H, 10% He and 10^{-4} heavy elements), turbulent
- magnetic fields (from galactic dynamo?)
- dust (solid phase, 1% mass compared to the gas), but (thermo)dynamically important...
- cosmic rays (high energy particles)

$$E_{th}=E_{grav}=E_{kin}=E_{mag}=E_{rad}=E_{cr} \sim 1 \text{ ev/cm}^3$$

➡ multifold research field, all processes couple together…

➡ slow progress

Magnetic fields are there, at all scales!

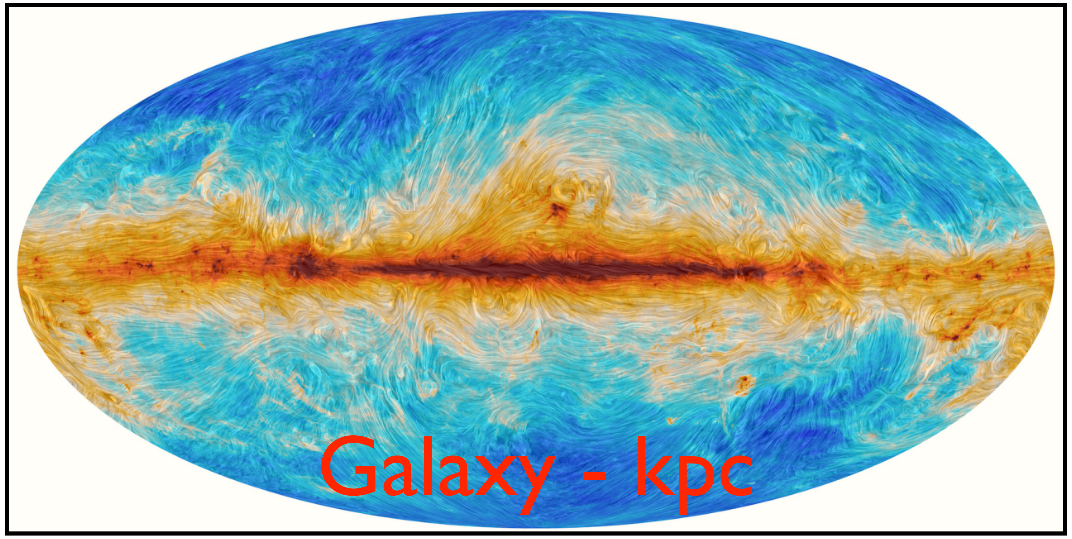

© ESA and the Planck Collaboration

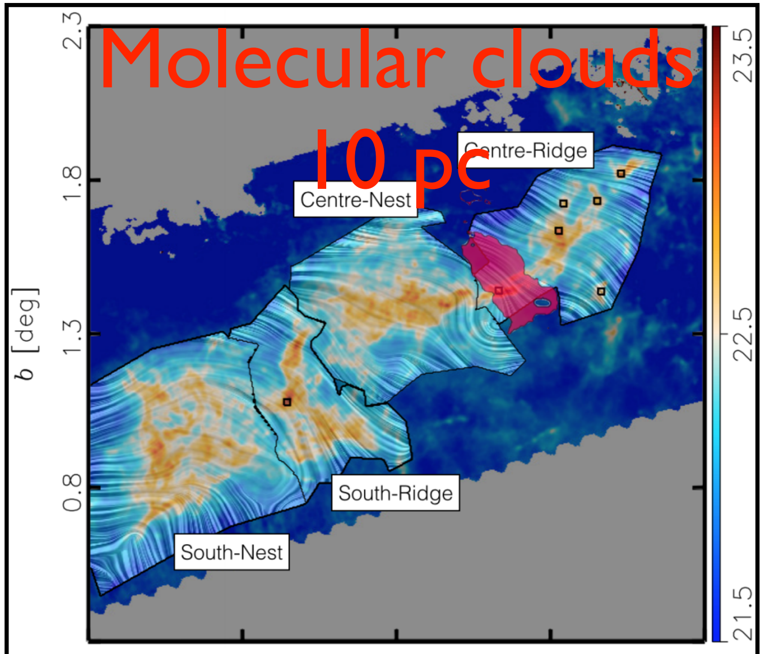

Soler et al. (2017, A&A) - BLASTPol

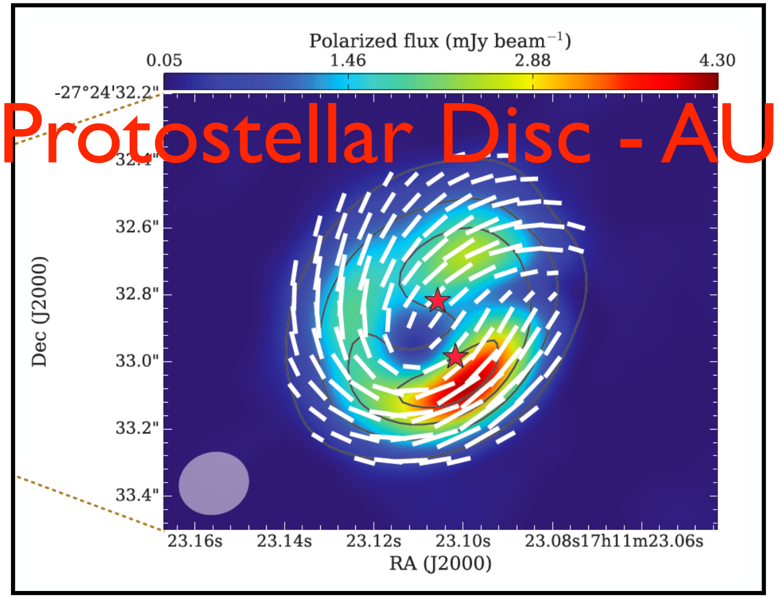

Alves et al. (2018, A&A) - ALMA

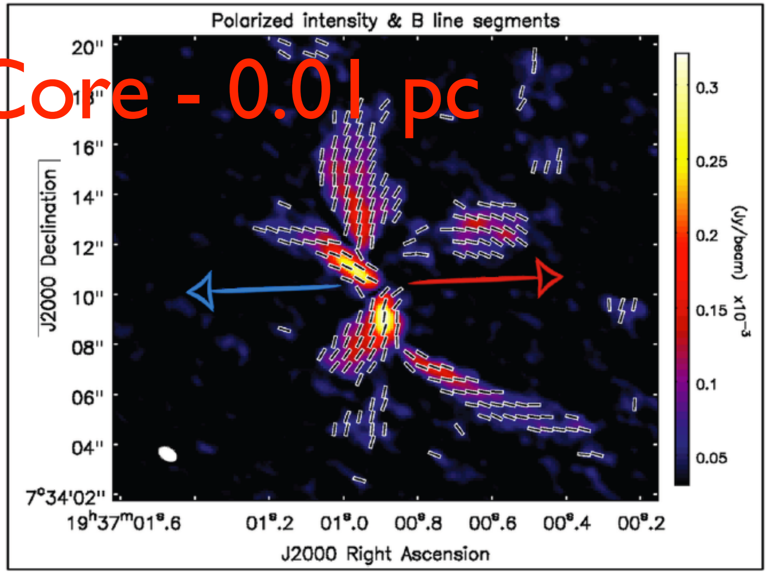

Maury et al. (2018) - ALMA

Molecular clouds are turbulent

Larson (1981) relations

$$n = 3000\ \mathrm{cm}^{-3} \left(\frac{L}{1\ \mathrm{pc}}\right)^{-0.7}$$

$$\Delta v_{\mathrm{NT}} \sim 1\ \mathrm{km\ s}^{-1} \left(\frac{L}{1\ \mathrm{pc}}\right)^{0.5}$$

$$\Delta v_{\mathrm{NT}} \sim 1\ \mathrm{km\ s}^{-1} \left(\frac{n}{3000\ \mathrm{cm}^{-3}}\right)^{-5/7}$$

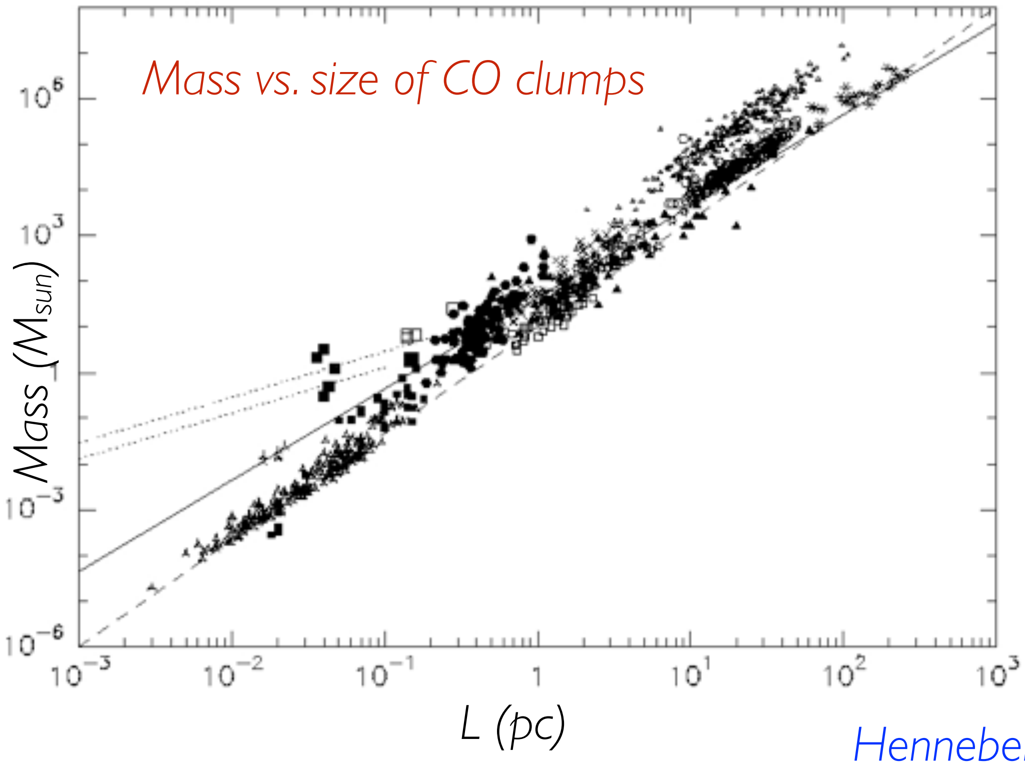

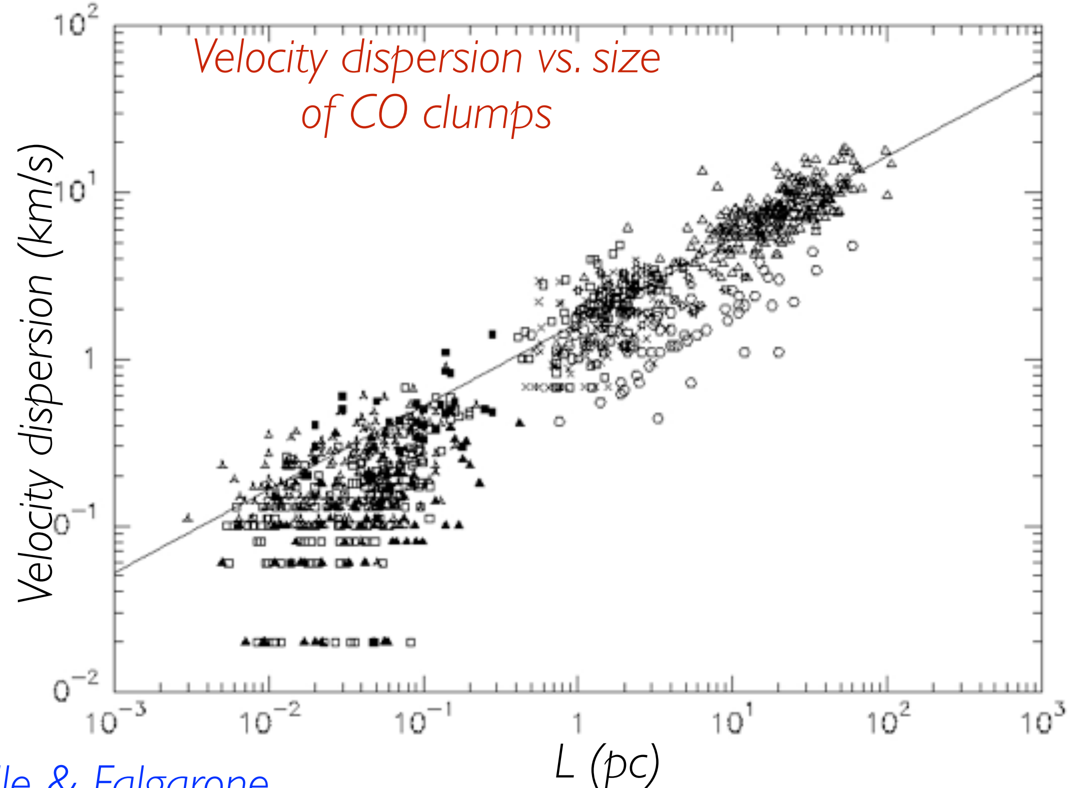

Hennebelle & Falgarone (2012 A&ARA)

Formation of self-gravitating cores

- **We now consider individual molecular clouds with:**
  - gravity
  - turbulence
  - magnetic field

- **Formation of gravitationally bound structures:**
  - Virial analysis, with only thermal support to balance gravity

$$2\mathcal{T} + \Omega = 0$$

$$M_{\rm crit} \propto \frac{C_{\rm s}^3}{\sqrt{n}}$$

Formation of self-gravitating cores

- **We now consider individual molecular clouds with:**
  - gravity
  - turbulence
  - magnetic field

- **Formation of gravitationally bound structures:**
  - Virial analysis, with only thermal support

$$M_{\rm crit} \sim 1.9 \left(\frac{T}{10\ \rm K}\right)^{3/2} \left(\frac{n}{10^4\ \rm cm^{-3}}\right)^{-1/2}\ \rm M_\odot$$

Formation of self-gravitating cores

- Turbulence
  - fluctuations at small scales compared to the Jeans scale

$$C_{\mathrm{s,eff}}^2 \simeq C_{\mathrm{s}}^2 + V_{\mathrm{rms}}^2/3$$

- Formation of gravitationally bound structures

$$M_{\mathrm{crit}} \propto \frac{C_{\mathrm{s,eff}}^3}{\sqrt{n}}$$

- Gravo-turbulent model (*Hennebelle & Chabrier, Padoan & Nordlund*)

Formation of self-gravitating cores

- **Stability in presence of a magnetic field**

$$2\mathcal{T} - 4\pi R^3 P_{\rm ext} - \frac{1}{R}\left(\frac{3}{5}GM^2 - \frac{1}{3}R^4 B^2\right) = 0$$

- Critical mass $$M_{\rm c} \sim \left(\frac{5}{9G}\right)^{1/2} \phi_{\rm B}$$
- $M > M_c$: "magnetically supercritical" cloud
- Magnetic fields "dilute" gravity:

$$2(E_{\rm th} + E_{\rm kin}) + E_{\rm grav}(1 - \mu^{-2})$$

Dense core formation

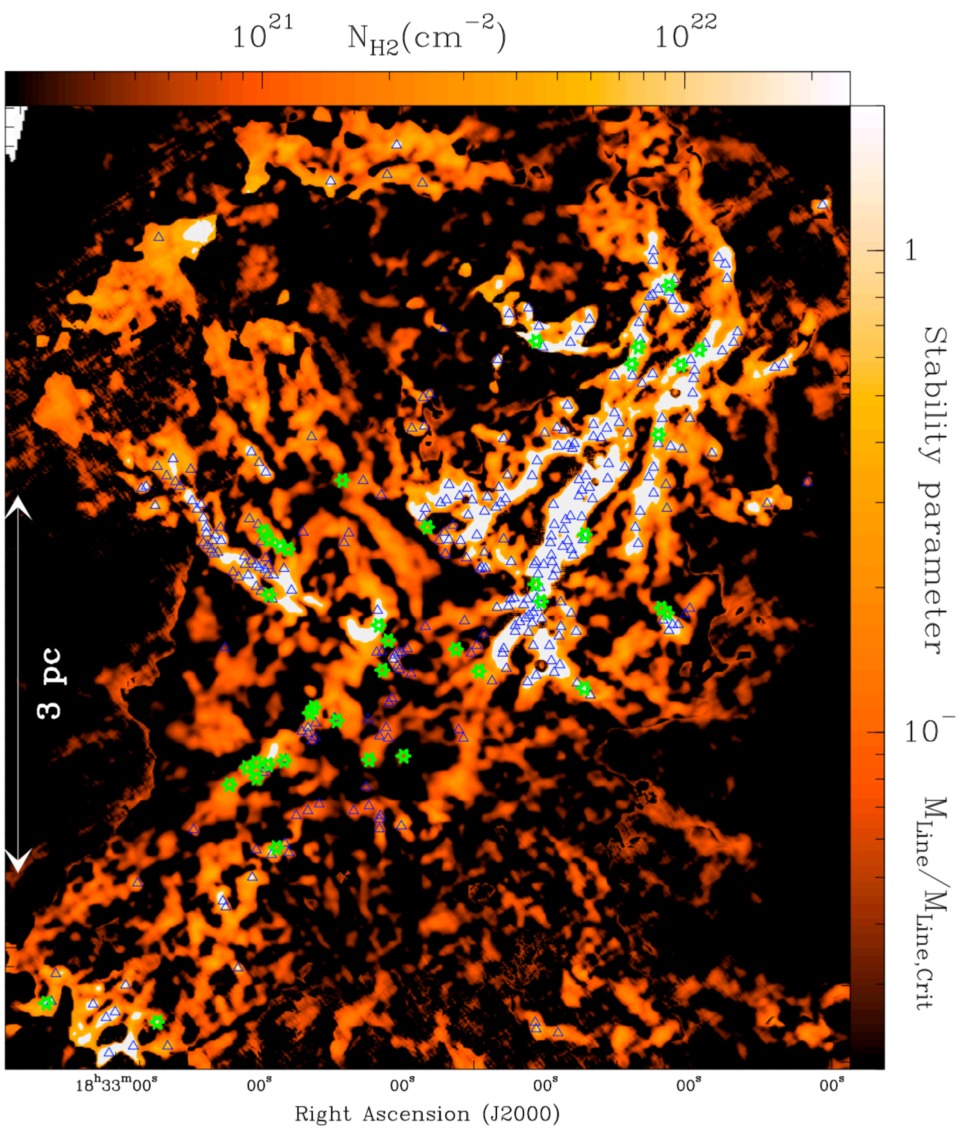

André et al. (2010)

- Within filaments and at the sonic scale for the majority
- Dense core are the progenitors of stars
- 1-1 relation between core mass function and stellar initial mass function?

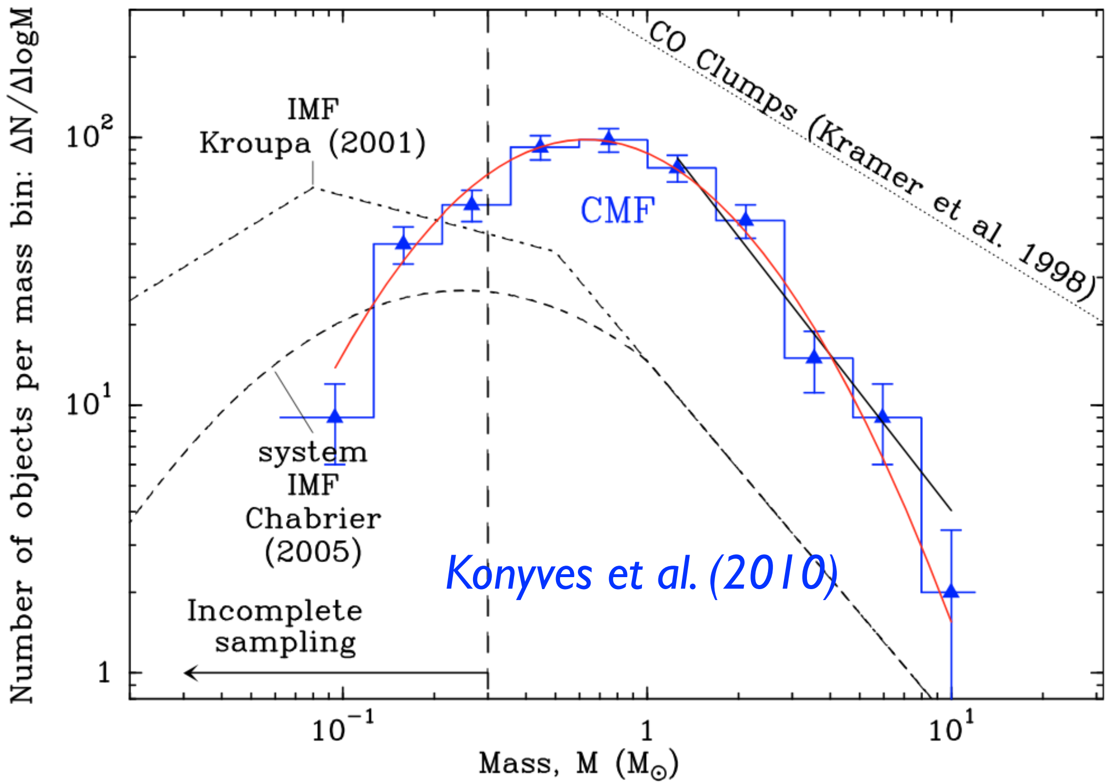

Dense core collapse: the challenge

✓ Follow the dynamics over a wide range of physical scales:

- time scales: free-fall time (~$10^{4,5}$ yr) to second
- spatial scales: parsec to stellar radius
- physical scales: density ranges form 10^4 cm^{-3} to 10^{24} cm^{-3}

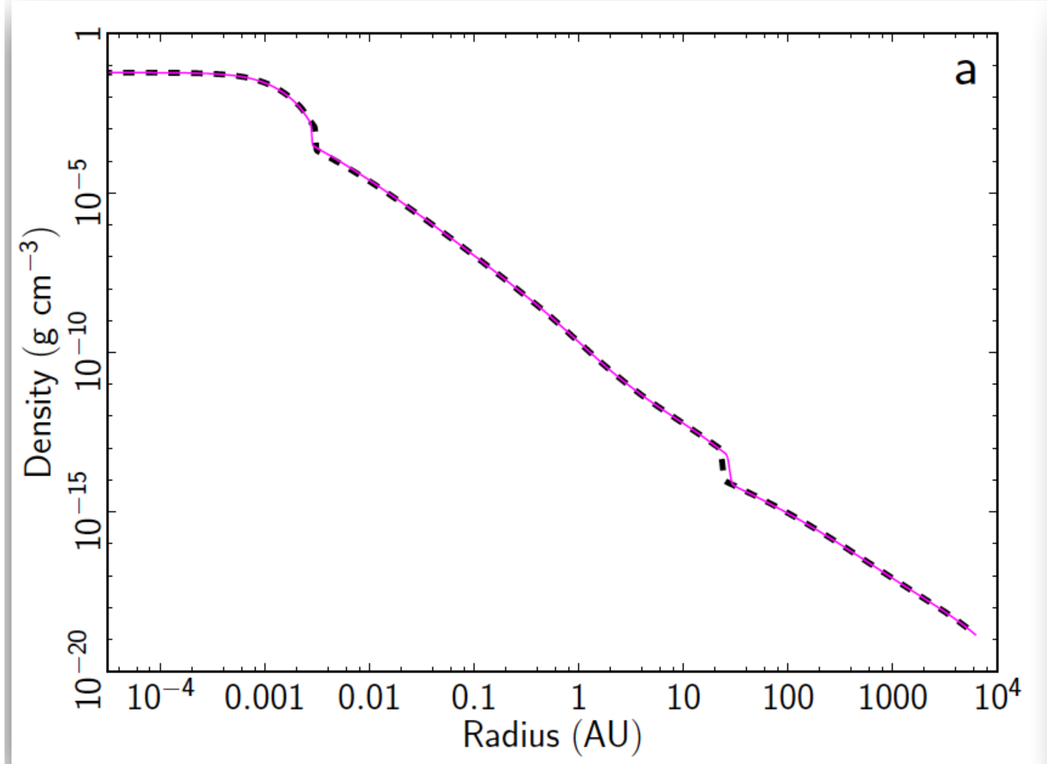

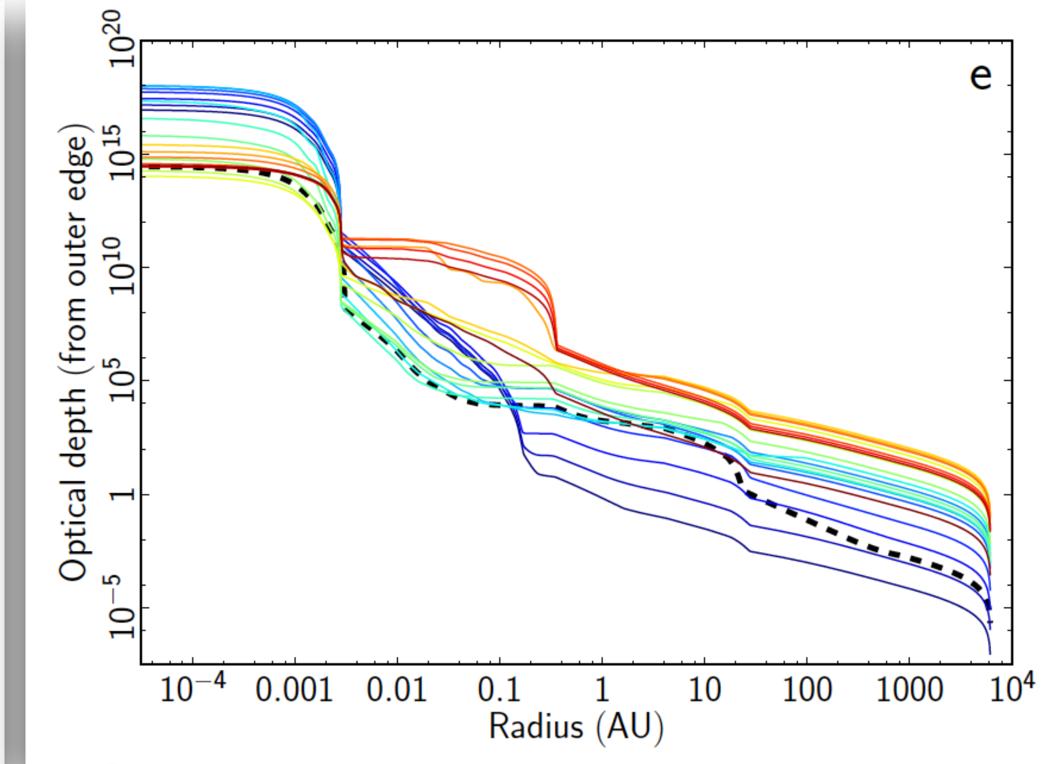

Vaytet et al. (2013)

Numerical tools for star formation

★ **3 numerical methods :**

– **Grid based** code - AMR: RAMSES, ENZO, FLASH

➡ Advantages :
- ✓ accuracy
- ✓ shocks
- ✓ refinement criteria

➡ Disadvantages :
- ✓ grid effects
- ✓ Eulerian
- ✓ complex structure

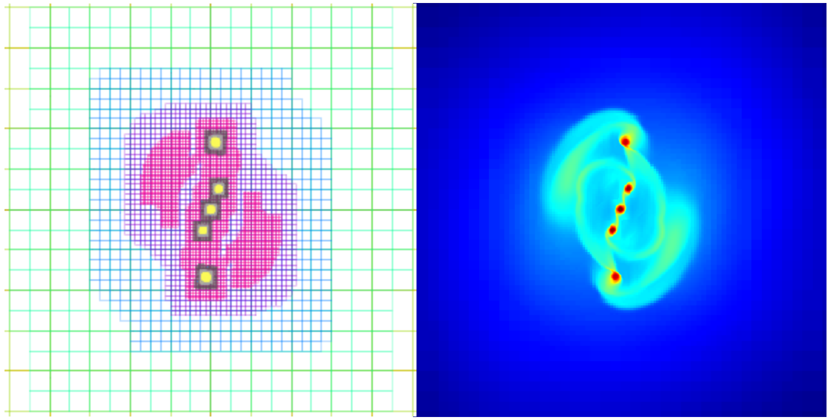

Numerical tools for star formation

★ 3 numerical methods :

– **Grid based code - AMR**: RAMSES, ENZO, FLASH

➡ Advantages :
- ✓ accuracy
- ✓ shocks
- ✓ refinement criteria

➡ Disadvantages :
- ✓ grid effects
- ✓ Eulerian
- ✓ complex structure

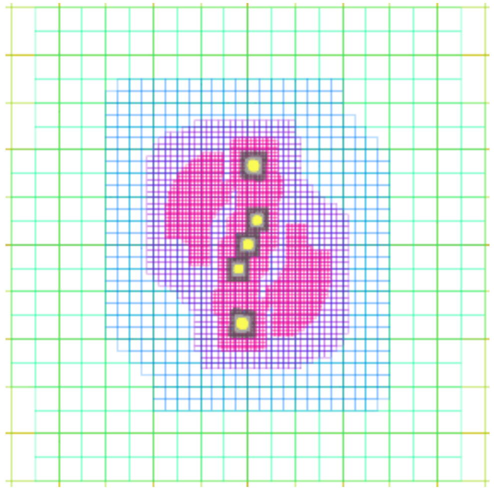

– **Smoothed Particle Hydrodynamics**: GADGET, PHANTOM, GASOLINE

➡ Advantages :
- ✓ Lagrangian
- ✓ naturally adaptive
- ✓ (simpler)

➡ Disadvantages :
- ✓ low density = low resolution
- ✓ noise, dissipative
- ✓ young

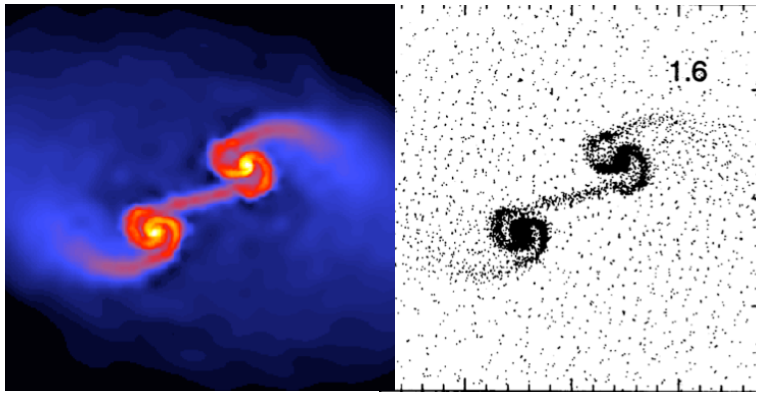

Numerical tools for star formation

★ 3 numerical methods :

– **Grid based code - AMR**: RAMSES, ENZO, FLASH

➡ Advantages :
- ✓ accuracy
- ✓ shocks
- ✓ refinement criteria

➡ Disadvantages :
- ✓ grid effects
- ✓ Eulerian
- ✓ complex structure

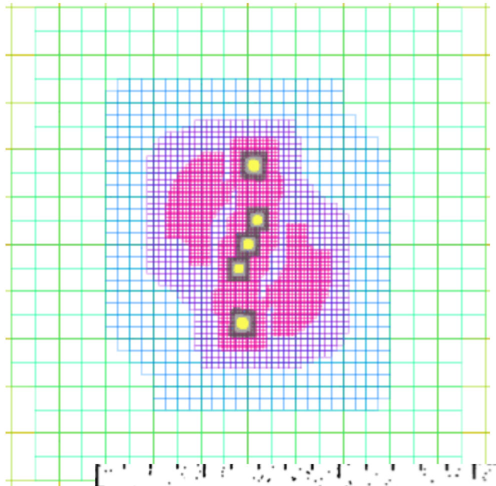

– **Smoothed Particle Hydrodynamics**: GADGET, PHANTOM, GASOLINE

➡ Advantages :
- ✓ Lagrangian
- ✓ naturally adaptive
- ✓ (simpler)

➡ Disadvantages :
- ✓ low density = low resolution
- ✓ noise, dissipative
- ✓ young

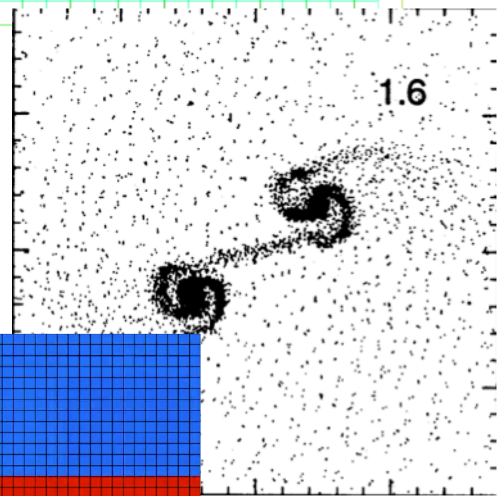

– Mix - Moving mesh: AREPO

➡ Advantages :
- ✓ Lagrangian/Eulerian
- ✓ naturally adaptive

➡ Disadvantages :
- ✓ Tessellation
- ✓ young

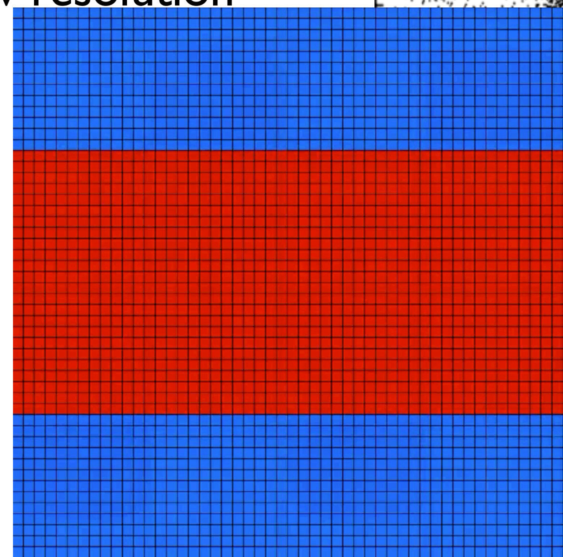

Take away I

Star forms in turbulent and magnetised molecular clouds

All components AND all scales of the ISM regulate the evolution of molecular clouds

Multi-scales and multi-physics tools

Outline

1. Introduction
2. **Dense core collapse, disc formation (pc to au)**
3. Formation of the protostar (au to $R_\odot$)
4. Observations
5. Perspectives

Star formation evolutionary sequence

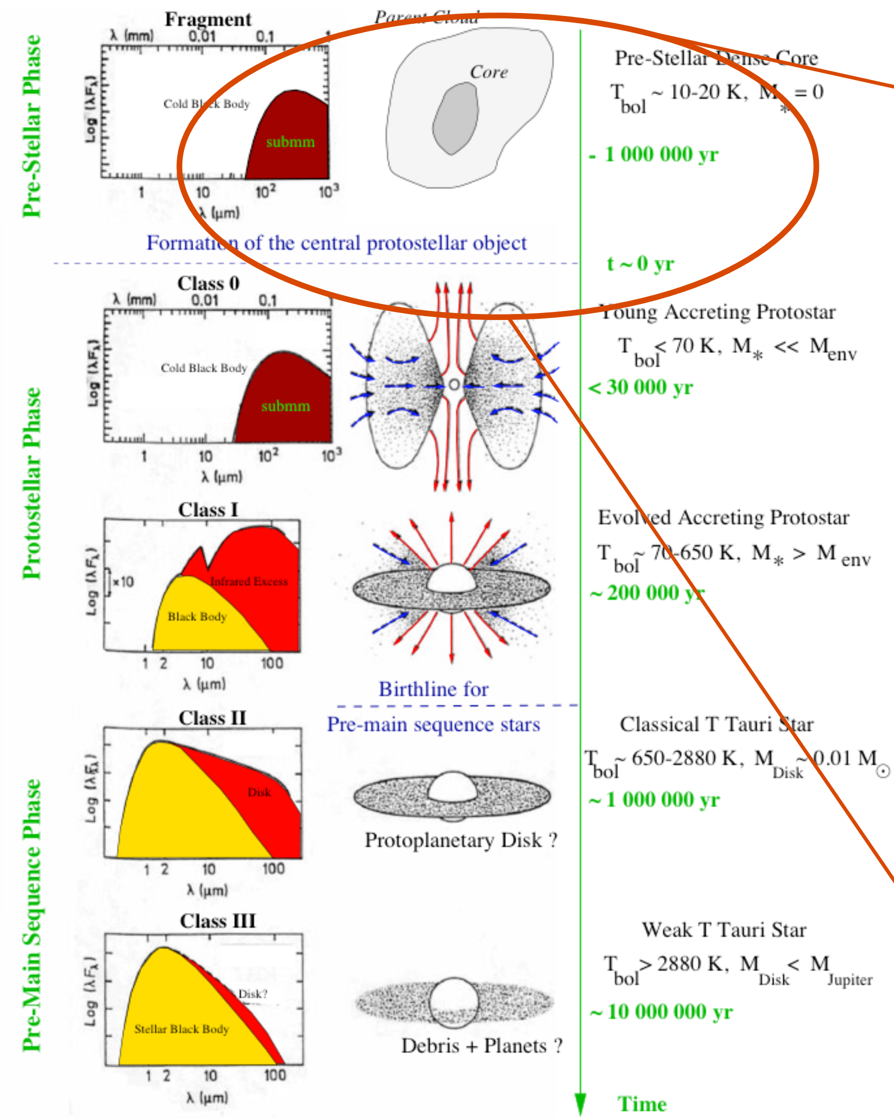

André 2002

Prestellar dense core collapse
(R=0.01 pc, T=10 K, n=10^6 cm^{-3})

First collapse

Isothermal — ***$10^{4,5}$ yr***

First Larson core

(R=10 AU, T=100 K, n=10^{12} cm^{-3})

Adiabatic — ***a few 10^3 yr***

H_2 dissociation

Second collapse

Quasi - isothermal — ***10^2 yr***

Second Larson core

(R=0.01 AU, T=10^{4-5} K, n=0.01cm^{-3})

Larson (1969)

Star formation evolutionary sequence

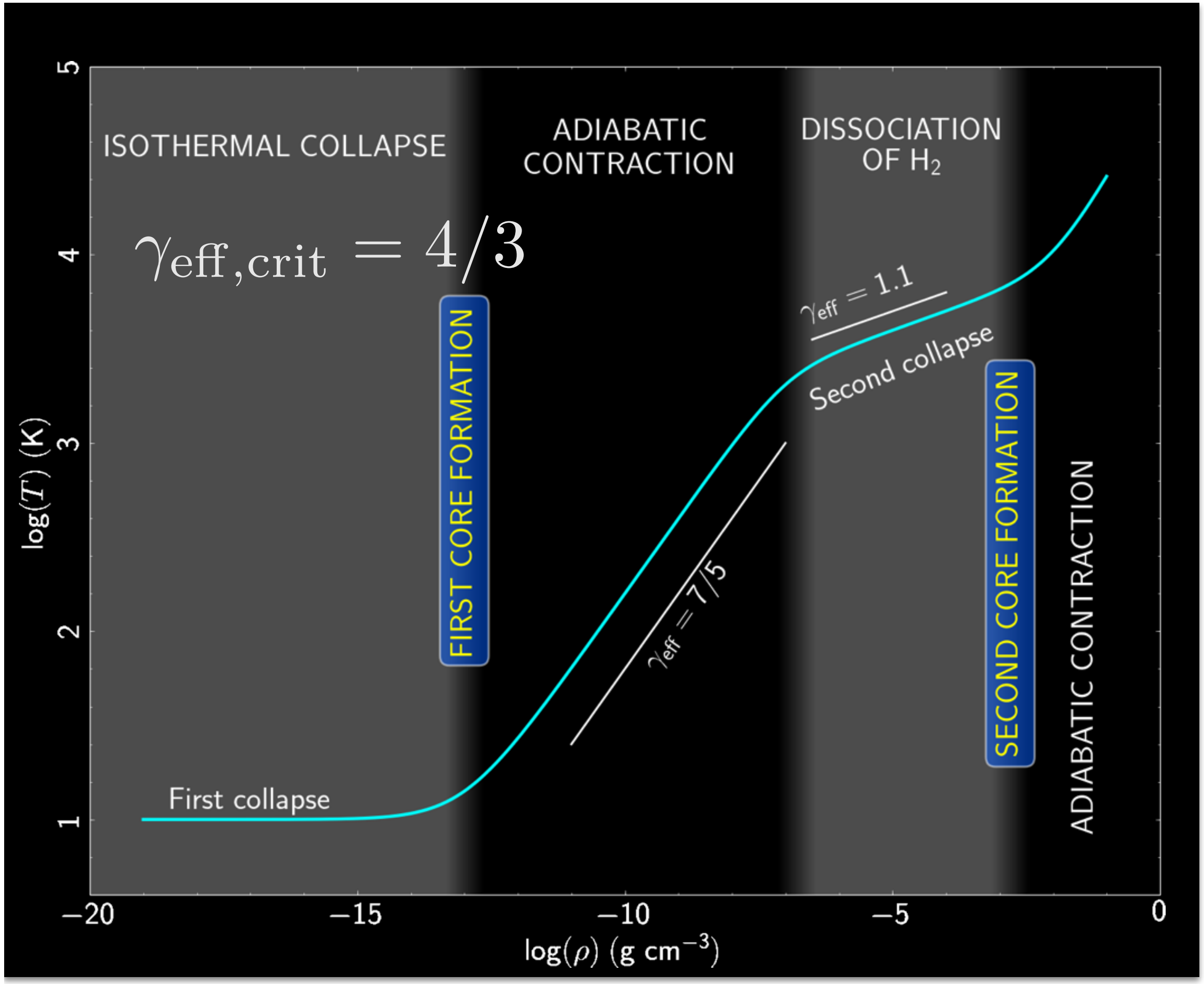

Vaytet et al. (2013)

$$M_{\rm Jeans} \propto \rho^{\frac{3\gamma_{\rm eff}}{2}-2} \quad \text{if} \quad P \propto \rho^{\gamma_{\rm eff}}$$

Prestellar dense core collapse
(R=0.01 pc, T=10 K, n=10^6 cm^{-3})

First collapse

Isothermal ↓ ***$10^{4,5}$ yr***

First Larson core
(R=10 AU, T=100 K, n=10^{12} cm^{-3})

Adiabatic ↓ ***a few 10^3 yr***

H_2 dissociation

Second collapse

Quasi - isothermal ↓ ***10^2 yr***

Second Larson core
(R=0.01 AU, T=$10^{4\text{-}5}$ K, n=0.01cm^{-3})

Larson (1969)

Protostar formation

- Formation of a very complex structure, with jets, outflows, discs, etc..
- Disc formation depends highly on MHD effects...
- Chemistry, cosmic rays have to be taken into account to estimate ionization

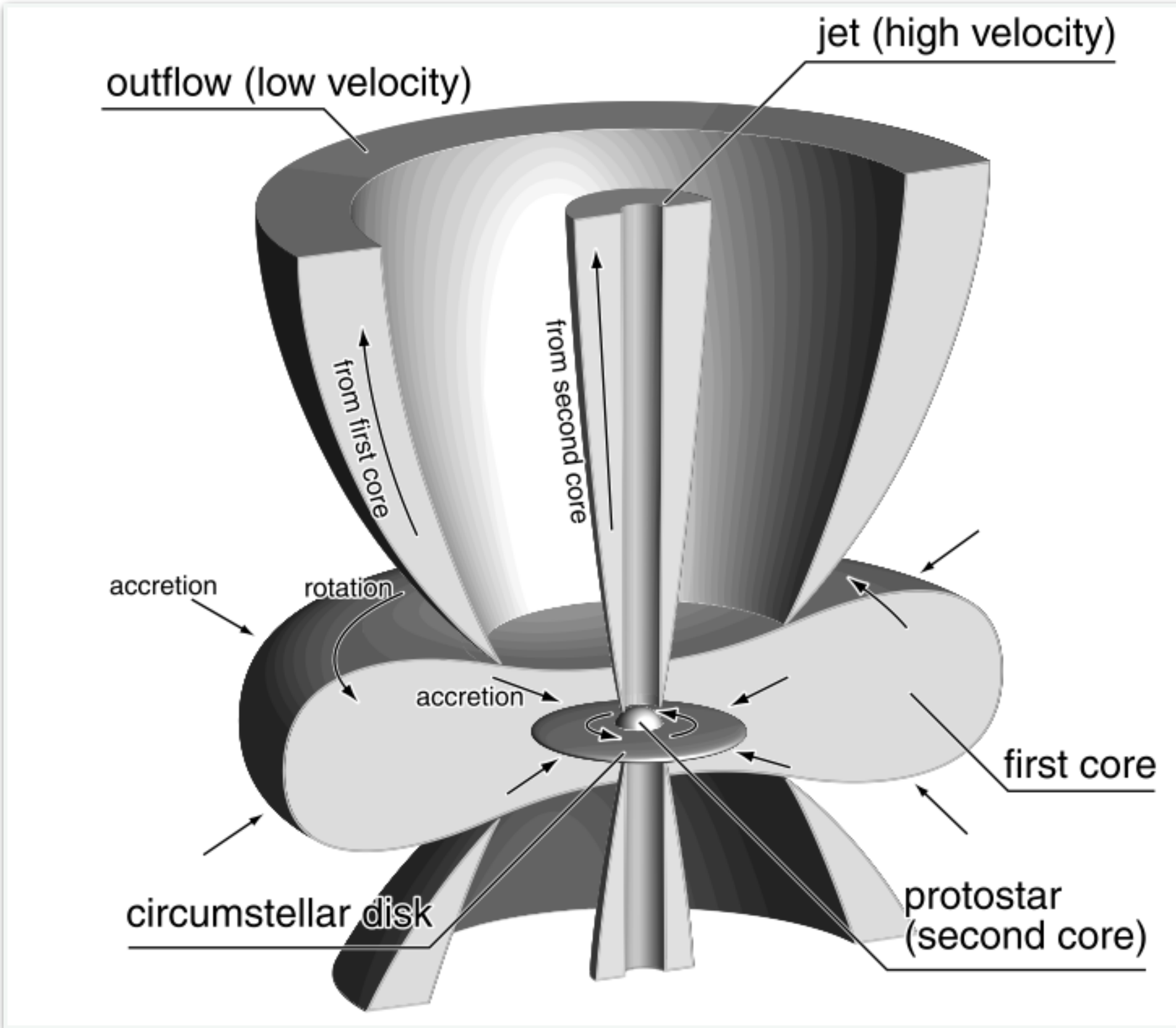

Machida et al. (2010)

Protostar formation

- Formation of a very complex structure, with jets, outflows, discs, etc..
- Disc formation depends highly on MHD effects...
- Chemistry, cosmic rays have to be taken into account to estimate ionization
- When does the disc form? Does it fragment?

➡ Implications for planet formation

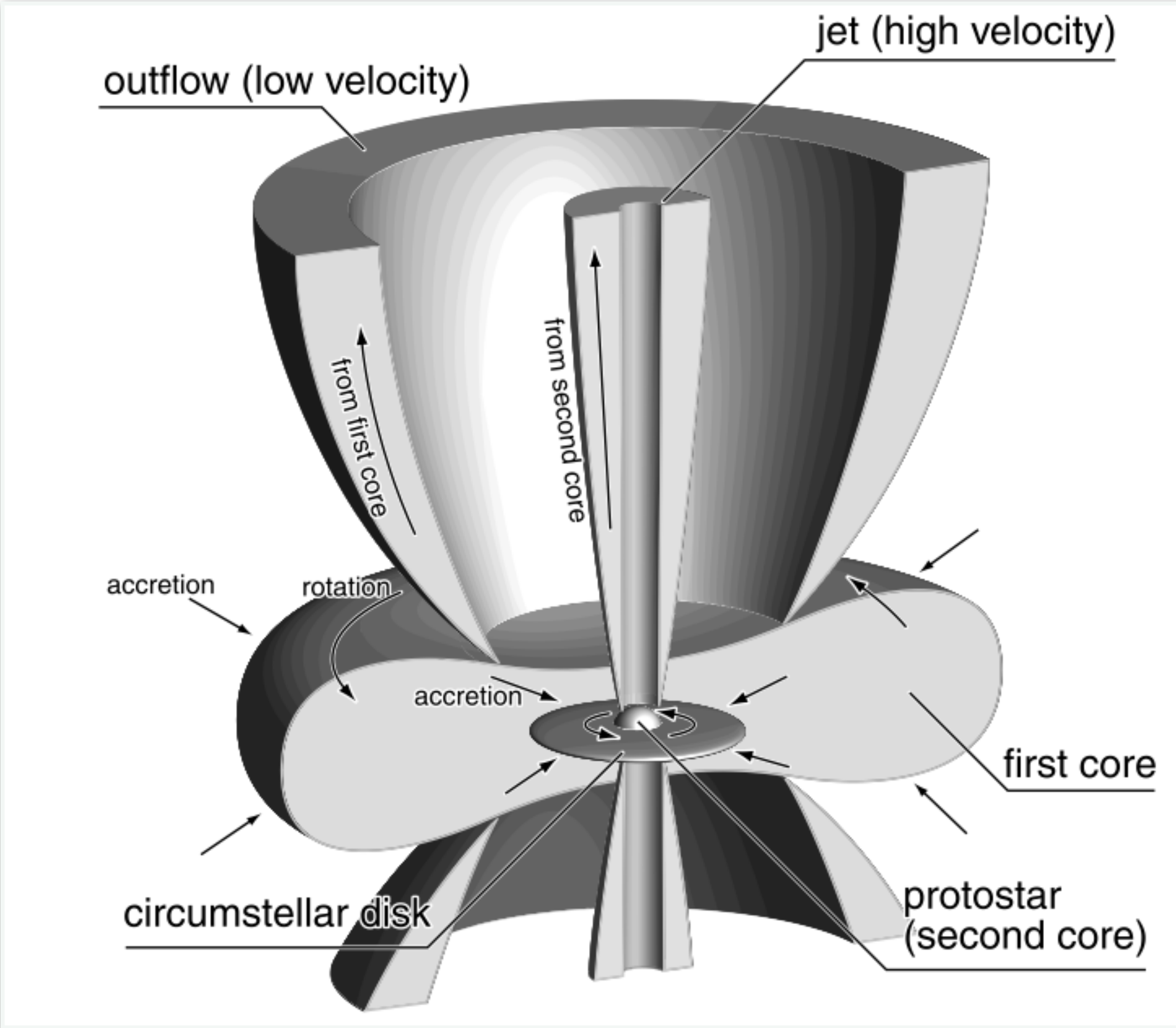

Machida et al. (2010)

Effect of magnetic fields and rotation

Consider a dense core of initial radius R, mass M and temperature T

Thermal support

- E_{th}/E_{grav} decreases when R decreases

$$\frac{E_{\rm th}}{E_{\rm grav}} = \frac{3M/m_p kT}{2GM^2/R} \propto R$$

Centrifugal support

- Angular momentum conservation
- E_{rot}/E_{grav} increases when R decreases

$$j = R_0^2 \omega_0 = R^2 \omega(t)$$

$$\frac{E_{\rm rot}}{E_{\rm grav}} = \frac{MR^2\omega^2}{GM^2/R} \propto \frac{1}{R}$$

Magnetic support

- Magnetic flux conservation
- E_{mag}/E_{grav} is constant when R decreases

$$\phi \propto BR^2$$

$\mu = (\varphi/M)_{crit}/(\varphi/M)$ (observations $\mu \sim$ 2-5)

$$\frac{E_{\rm mag}}{E_{\rm grav}} = \frac{B^2R^3}{GM^2/R} \propto \left(\frac{\phi}{M}\right)^2$$

Effect of magnetic fields and rotation

Consequences:

Centrifugal forces become dominant

- flattening of the envelope
- formation of a centrifugally supported disc

Magnetic forces stay comparable to gravity

- flattening of the envelope
- NO formation of a supported structure
- formation of a pseudo-disc (Galli & Shu 1993)

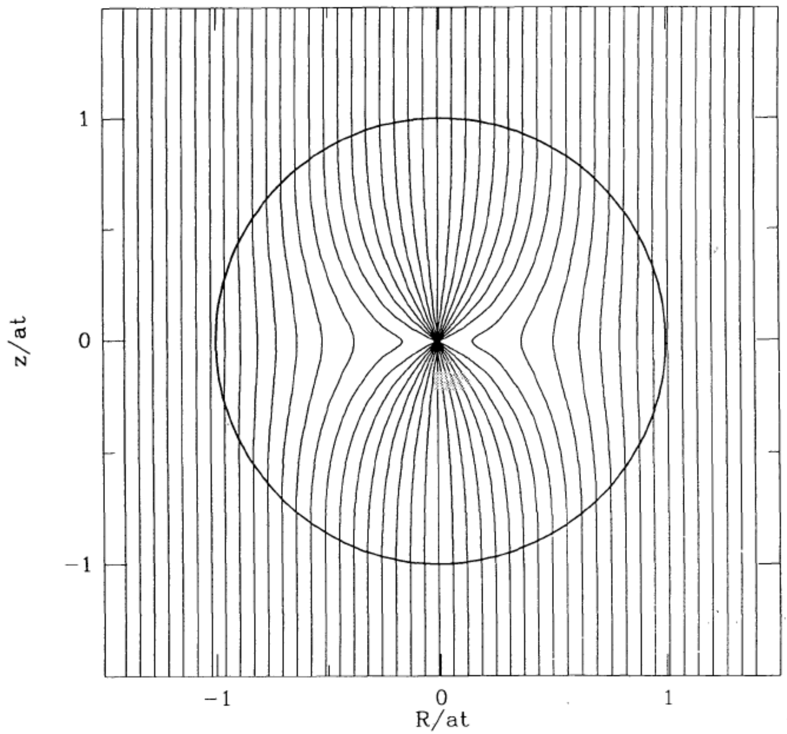

Galli & Shu 1993

Magnetic fields brakes the cloud

- transfer angular momentum from the inner part to the envelop

Angular momentum conservation

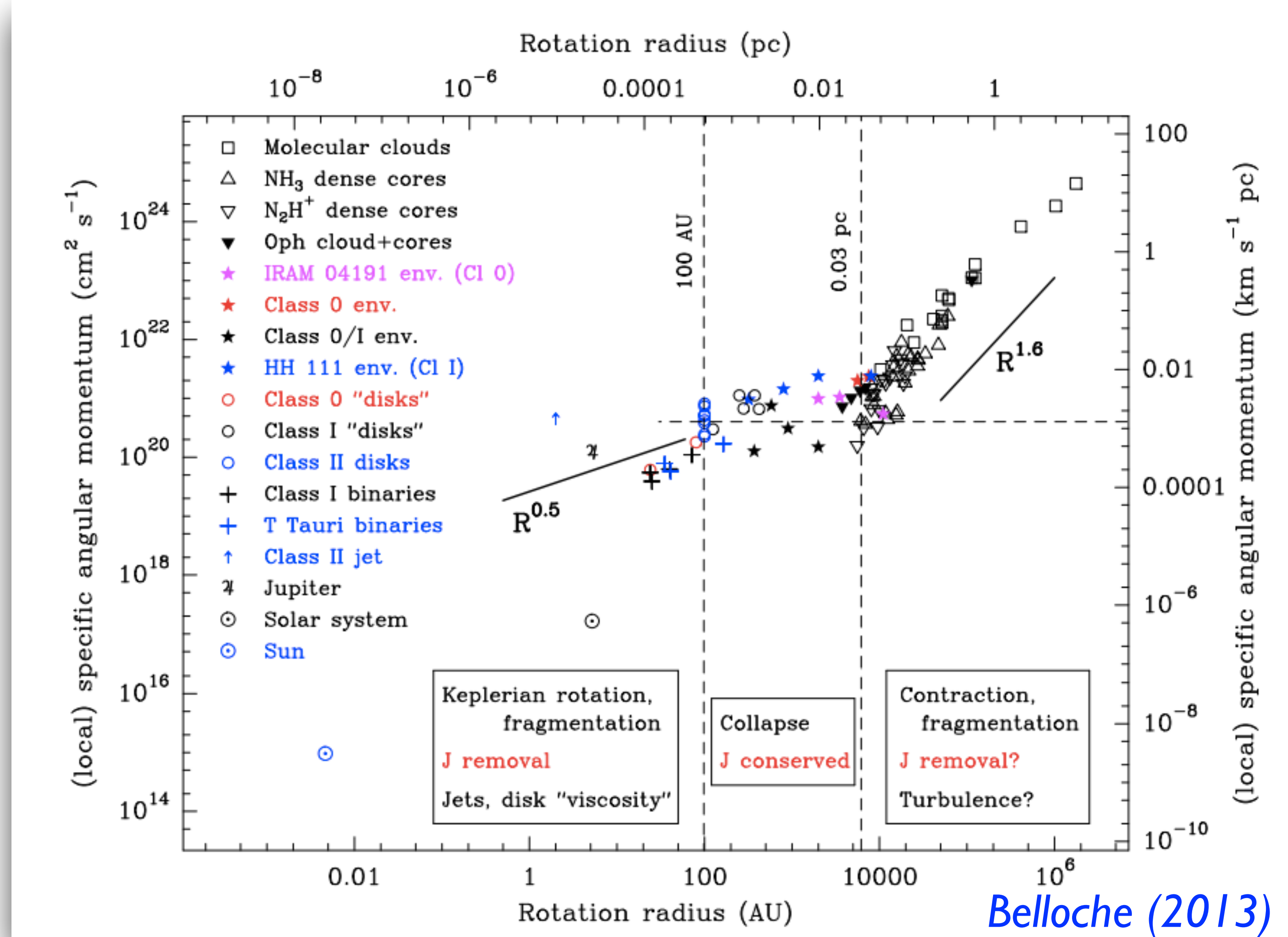

Belloche (2013)

Magnetic flux problem

Consider a cloud of initial radius R=0.1 pc, B~ 10 μG

- ✓ Magnetic flux $\Phi=\pi BR^2 \sim 3\times10^{32}$ G cm^2
- ✓ if flux is conserved, at a solar radius (6.5×10^{10} cm), B~ 10^{10} G

➡ Magnetic field in star is observed to be < 10^4 G

=> Magnetic flux has to be removed or transported away during gravitational collapse

Numerical experiments

Typical initial conditions:

- 1 - 100s $M_\odot$ isolated dense core
- uniform / BE-like density profile
- uniform temperature (10 K, $\alpha = E_{th}/E_{grav}$)
- solid body / differential rotation ($\beta = E_{rot}/E_{grav}$)
- m=2 density perturbation / turbulent velocity field
- organised magnetic field

$\mu = (\varphi/M)_{crit} / (\varphi/M)$ (observations $\mu \sim 2$-5)

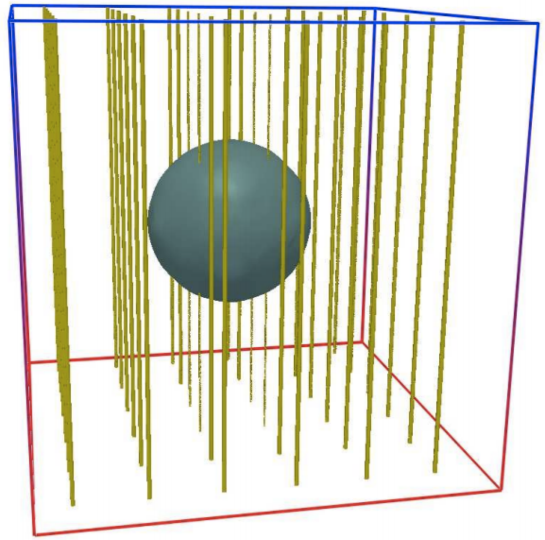

Banerjee & Pudritz (2006)

Refinement criterion solely based on the Jeans length

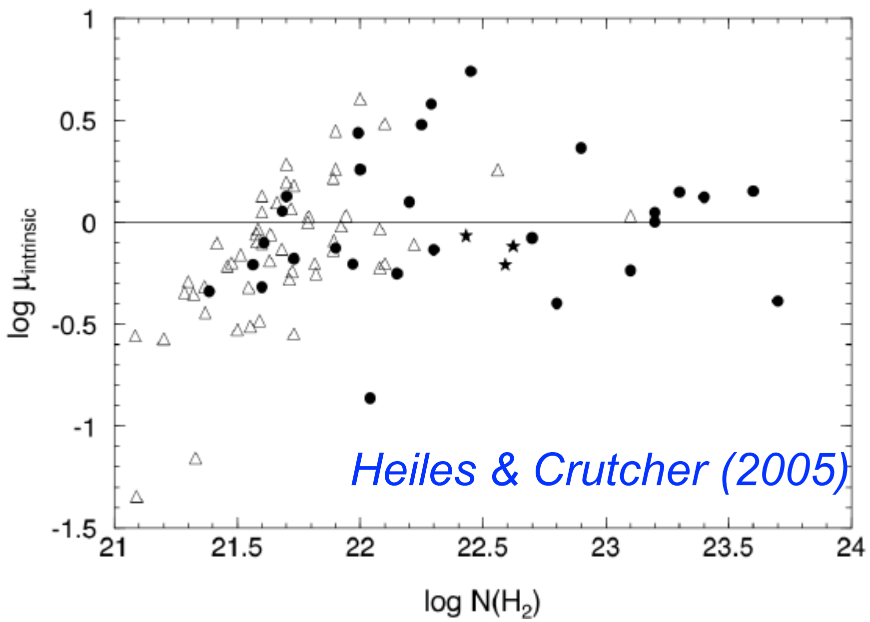

Heiles & Crutcher (2005)

State-of-the-art in 2008: ideal MHD in 1 Msun core

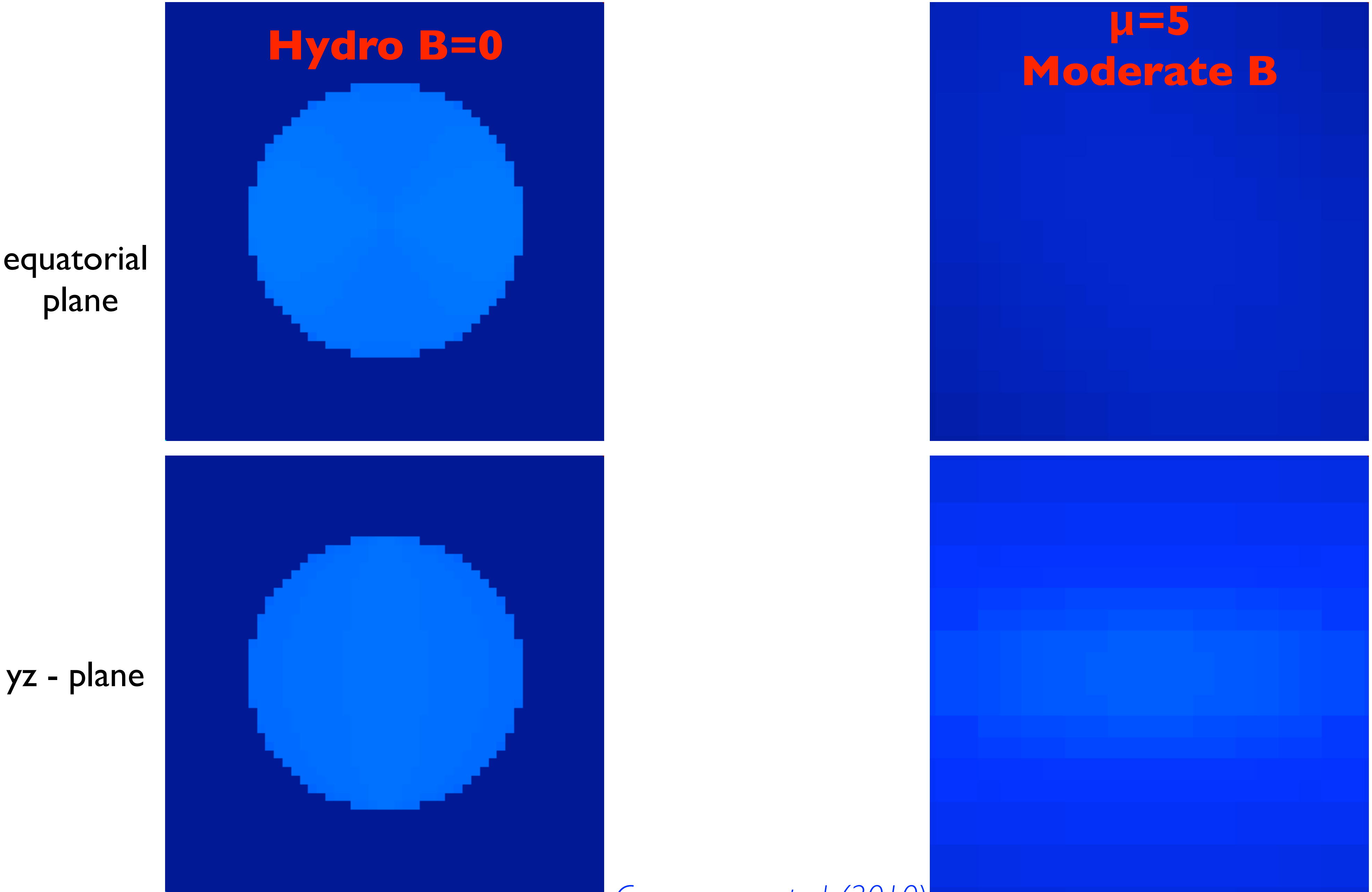

Commerçon et al. (2010)

State-of-the-art in 2008: ideal MHD in 1 Msun core

Magnetic braking

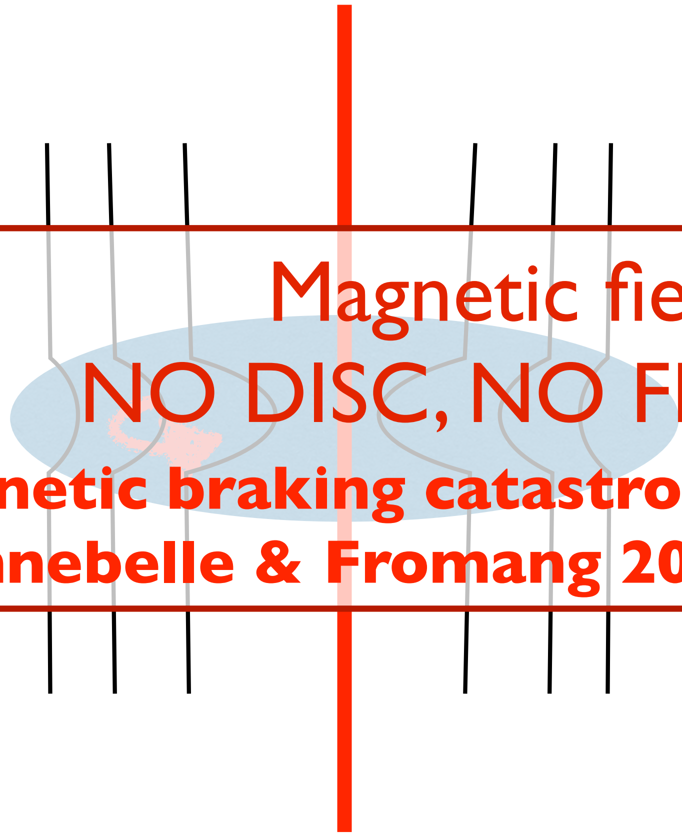

μ=5
Moderate B

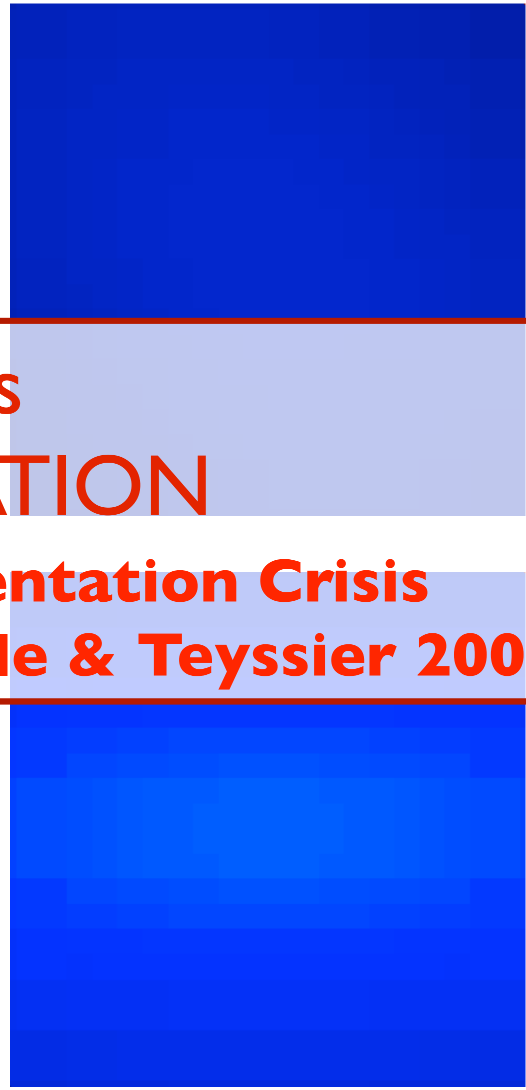

Magnetic field dominates

NO DISC, NO FRAGMENTATION

Magnetic braking catastrophe & Fragmentation Crisis
(e.g., Hennebelle & Fromang 2008, Hennebelle & Teyssier 2008)

Commerçon et al. (2010)

Disc formation in magnetised cores

- ✓ **Late formation**
  - ➢ end of class 0, $M_{env} << M_{env,0}$ (e.g., *Machida & Hosokawa 2013*)

- ✓ **Misalignment**
  - ➢ no reason for the rotation axis and the magnetic field to be aligned (e.g., *Hull et al. 2013*)
  - ➢ reduces magnetic braking efficiency (e.g. *Hennebelle & Ciardi 2009, Joos et al. 2012, Li et al. 2013*)

- ✓ **Turbulent reconnection**
  - ➢ reconnection events at small scales are fast with Ohmic diffusion only, collective effect at larger scale (e.g. *Santos Lima et al. 2012, Joos et al. 2013, Seifried et al. 2013*)

- ✓ **Non-ideal MHD**
  - ➢ Ohmic dissipation (*Tomida et al. 2013, 2015, Machida et al.*)
  - ➢ Hall effect (*Krasnopolsky et al. 2011, Tsukamoto et al. 2015, 2017, Wurster et al. 2016, 2018, Marchand et al. 2018, 2019*)
  - ➢ ambipolar diffusion (*Tsukamoto et al. 2015, Masson et al. 2016, Wurster et al.*)

Disc formation in magnetised cores

- ✓ Late formation
  - end of class 0, $M_{env} << M_{env,0}$ (e.g., *Machida & Hosokawa 2013*)
- ✓ Misalignment
  - no reason for the rotation axis and the magnetic field to be aligned (e.g., *Hull et al. 2013*)
  - reduces magnetic braking efficiency (e.g. *Hennebelle & Ciardi 2009, Joos et al. 2012, Li et al. 2013*)
- ✓ Turbulent reconnection
  - reconnection events at small scales are fast with Ohmic diffusion only, collective effect at larger scale (e.g. *Santos Lima et al. 2012, Joos et al. 2013, Seifried et al. 2013*)
- ✓ Non-ideal MHD
  - Ohmic dissipation (*Tomida et al. 2013, 2015, Machida et al.*)
  - Hall effect (*Krasnopolsky et al. 2011, Tsukamoto et al. 2015, 2017, Wurster et al. 2016, 2018, Marchand et al. 2018, 2019*)
  - ambipolar diffusion (*Tsukamoto et al. 2015, Masson et al. 2016, Wurster et al.*)

Non-ideal MHD

Ohmic diffusion — Hall effect — Ambipolar diffusion

$$\frac{\partial \mathbf{B}}{\partial t} - \nabla \times \left[\mathbf{u} \times \mathbf{B} - \eta_{\Omega} \mathbf{J} - \frac{\eta_{\mathrm{H}}}{||\mathbf{B}||} \mathbf{J} \times \mathbf{B} + \frac{\eta_{\mathrm{AD}}}{||\mathbf{B}||^2} \mathbf{J} \times \mathbf{B} \times \mathbf{B} \right] = 0$$

Non-ideal effects:

- rearrangement of magnetic field lines
- reconnection
- magnetic flux diffusion
- … needs **gas-grain chemistry**

✓ Non-ideal MHD

- Ohmic dissipation (*Tomida et al. 2013, 2015, Machida et al.*)
- Hall effect (*Krasnopolsky et al. 2011, Tsukamoto et al. 2015, 2017, Wurster et al. 2016, 2018, Marchand et al. 2018, 2019*)
- ambipolar diffusion (*Tsukamoto et al. 2015, Masson et al. 2016, Wurster et al.*)

Equilibrium chemistry for non-ideal MHD

✓ **Reduced chemical network dedicated for ionisation (based on the work by *Umebayashi & Nakano 1990*)**

- H, He, C, O, metallic elements (Fe, Na, Mg, etc..)
- H^+, $H_3{}^+$, He^+, C^+, molecular and metallic ions
- bins in the dust grains size distribution (G, G^+, G^-)
- dust evaporation at T>800 K
- thermal ionisation of potassium (T>1000 K)
- neutral elements have constant abundances

Reaction	α	β	γ
$H^+ + O \rightarrow H + O^+$	6.86×10^{-10}	0.26	0
$H^+ + O_2 \rightarrow H + O_2^+$	2.00×10^{-9}	0.00	0
$H^+ + M \rightarrow H + M^+$	1.10×10^{-9}	0.00	0
$He^+ + H_2 \rightarrow He + H^+ + H$	3.70×10^{-14}	0.00	35
$He^+ + CO \rightarrow He + C^+ + O$	1.60×10^{-9}	0.00	0
$He^+ + O_2 \rightarrow He + O^+ + O$	1.10×10^{-9}	0.00	0
$H_3^+ + CO \rightarrow H_2 + HCO^+$	1.36×10^{-9}	−0.14	0
$H_3^+ + O \rightarrow H_2 + OH^+$	7.98×10^{-10}	−0.16	0
$H_3^+ + O_2 \rightarrow H_2 + O_2H^+$	9.30×10^{-10}	0.00	0
$H_3^+ + M \rightarrow H_2 + H + M^+$	1.10×10^{-9}	0.00	0
$C^+ + H_2 \rightarrow CH_2^+ + h\nu$	2.00×10^{-16}	0.00	0
$C^+ + O_2 \rightarrow CO^+ + O$	3.42×10^{-10}	0.00	0
$C^+ + O_2 \rightarrow CO + O^+$	4.54×10^{-10}	0.00	0
$C^+ + M \rightarrow C + M^+$	1.10×10^{-9}	0.00	0
$m^+ + M \rightarrow m + M^+$	2.90×10^{-9}	0.00	0
$H^+ + e^- \rightarrow H + h\nu$	3.50×10^{-12}	−0.75	0
$He^+ + e^- \rightarrow He + h\nu$	5.36×10^{-12}	−0.5	0
$H_3^+ + e^- \rightarrow H + H + H$; $\rightarrow H_2 + H$	2.34×10^{-8}	−0.52	0
$C^+ + e^- \rightarrow C + h\nu$	2.36×10^{-12}	−0.29	0
$m^+ + e^- \rightarrow m_1 + m_2$	2.40×10^{-7}	−0.69	0
$M^+ + e^- \rightarrow M + h\nu$	2.78×10^{-12}	−0.68	0
$H_2 \rightarrow H_2^+ + e^-$	1.2×10^{-17}		
$H_2 \rightarrow H^+ + H + e^-$	2.86×10^{-19}		
$He \rightarrow He^+ + e^-$	6.58×10^{-18}		

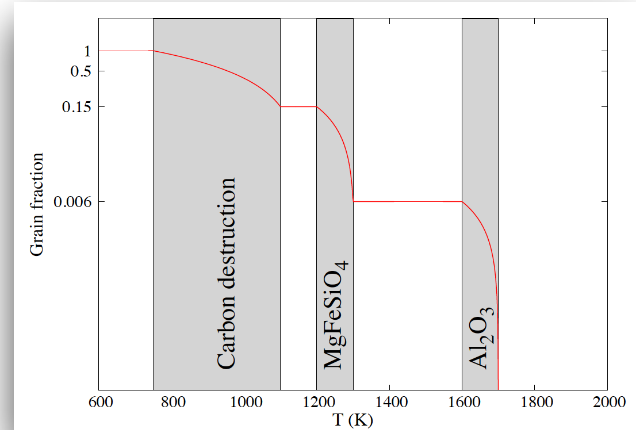

✓UMIST database for gas species (*McElroy et al. 2013*)

✓*Kunz & Mouschovias (2009)* for interactions with and between grains

✓ **Goal: compute a 3D table of abundances:**

- depends on temperature, density and CR ionisation

Marchand et al. (2016)

Equilibrium chemistry for non-ideal MHD

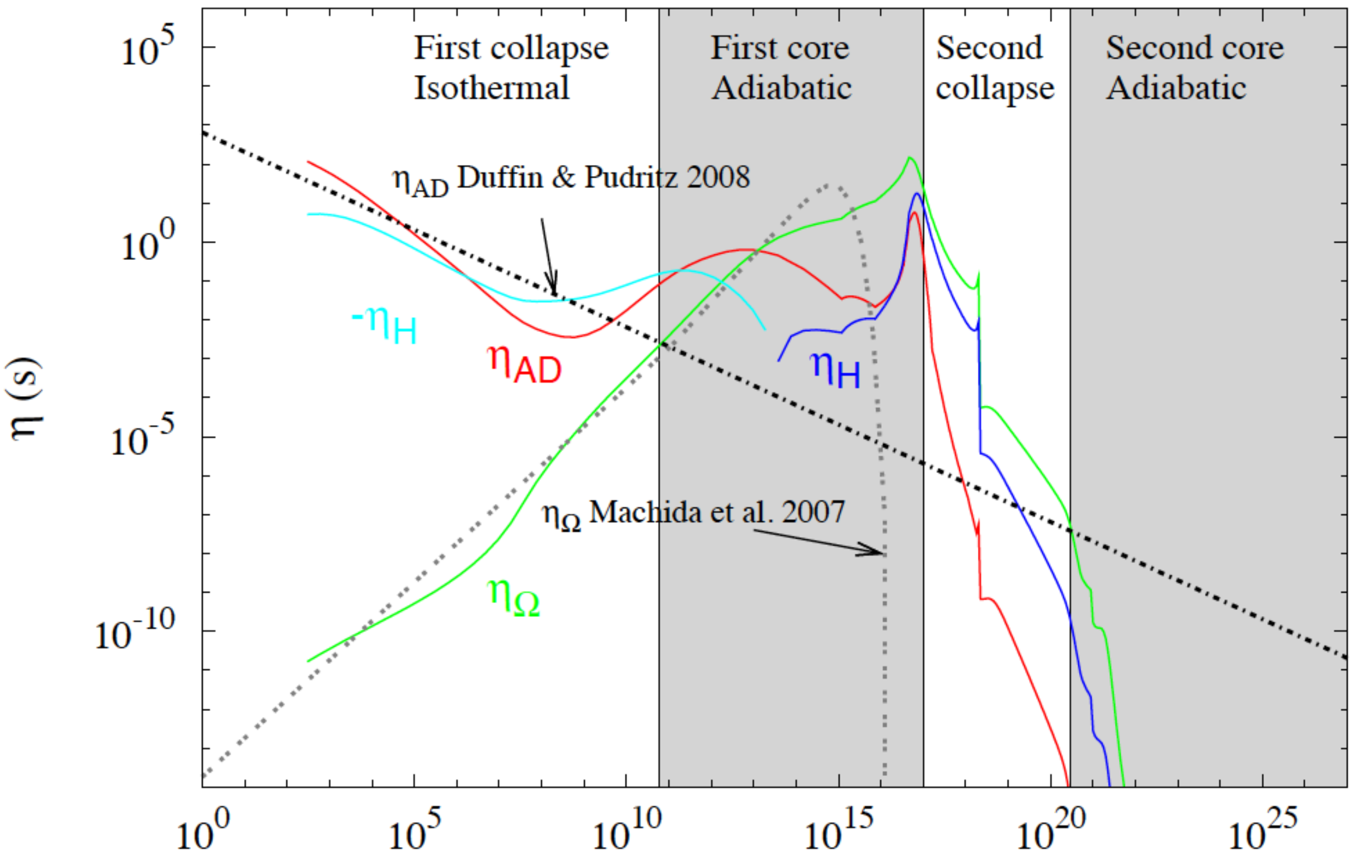

https://bitbucket.org/pmarchan/chemistry *Marchand et al. (2016)*

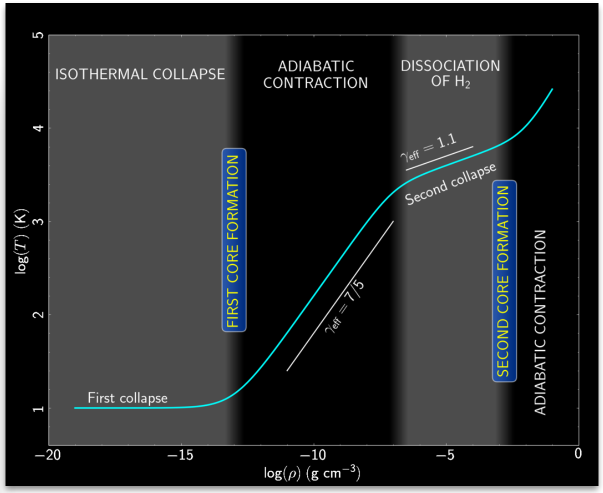

$$\sigma_{\parallel} = \sum_i \sigma_i,$$

$$\sigma_{\perp} = \sum_i \frac{\sigma_i}{1 + (\omega_i \tau_{in})^2},$$

$$\sigma_{H} = -\sum_i \frac{\sigma_i \omega_i \tau_{in}}{1 + (\omega_i \tau_{in})^2}.$$

$$\eta_{\Omega} = \frac{1}{\sigma_{\parallel}},$$

$$\eta_{H} = \frac{\sigma_H}{\sigma_{\perp}^2 + \sigma_H^2},$$

$$\eta_{AD} = \frac{\sigma_{\perp}}{\sigma_{\perp}^2 + \sigma_H^2} - \frac{1}{\sigma_{\parallel}},$$

1/ **Grain evaporation** is the most important effect

2/ Needs at least **5 bins** in dust grain size distribution to converge…

See *also Wurster (2016), Zhao et al. (2016, 2018), Dzyurkevich et al. (2017)*

Equilibrium chemistry for non-ideal MHD: results

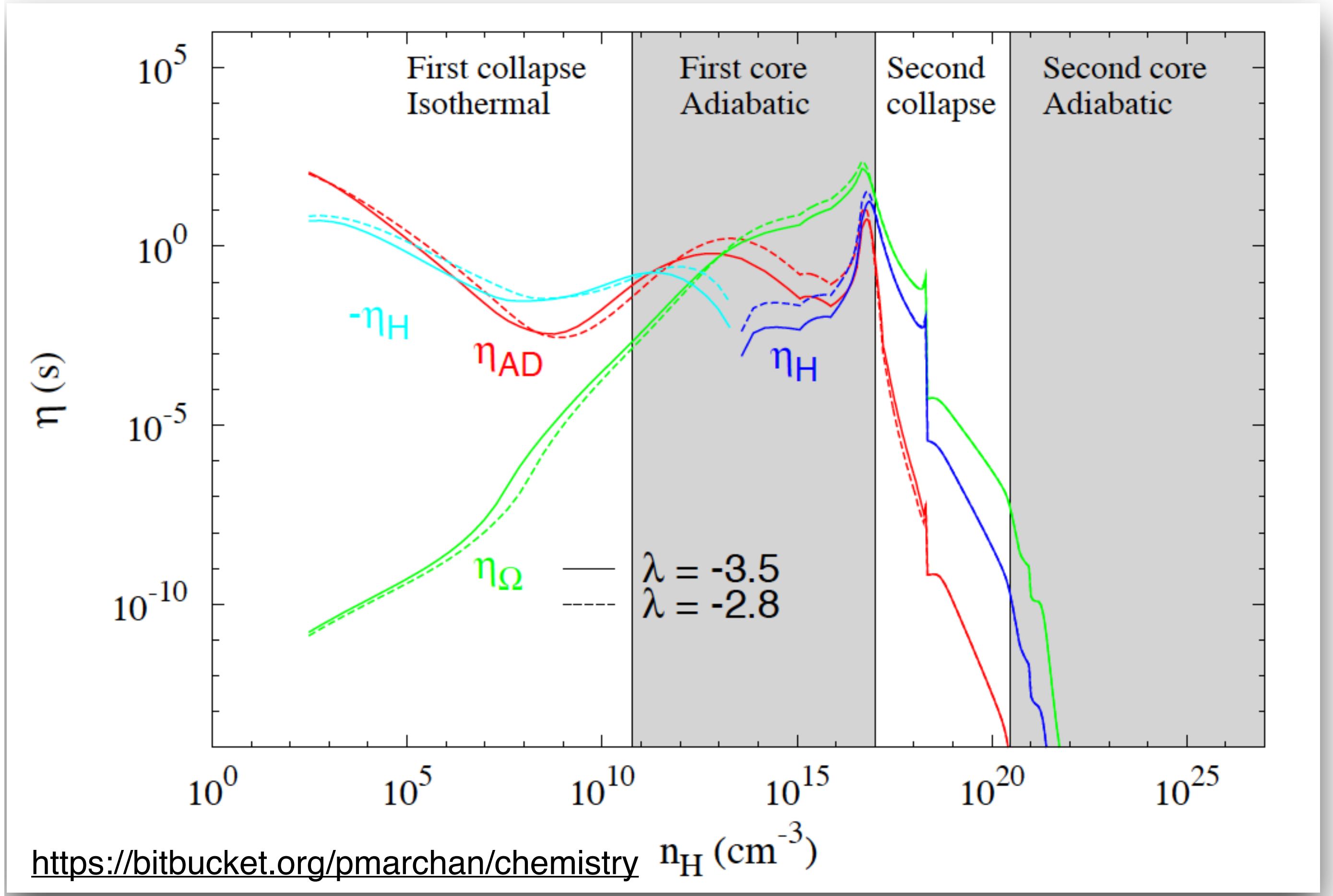

$$\sigma_\parallel = \sum_i \sigma_i,$$

$$\sigma_\perp = \sum_i \frac{\sigma_i}{1+(\omega_i \tau_{in})^2},$$

$$\sigma_H = -\sum_i \frac{\sigma_i \omega_i \tau_{in}}{1+(\omega_i \tau_{in})^2}.$$

$$\eta_\Omega = \frac{1}{\sigma_\parallel},$$

$$\eta_H = \frac{\sigma_H}{\sigma_\perp^2 + \sigma_H^2},$$

$$\eta_{AD} = \frac{\sigma_\perp}{\sigma_\perp^2 + \sigma_H^2} - \frac{1}{\sigma_\parallel},$$

Grain size distribution as first-order effect

Marchand et al. (2016)

Cosmic rays ionisation

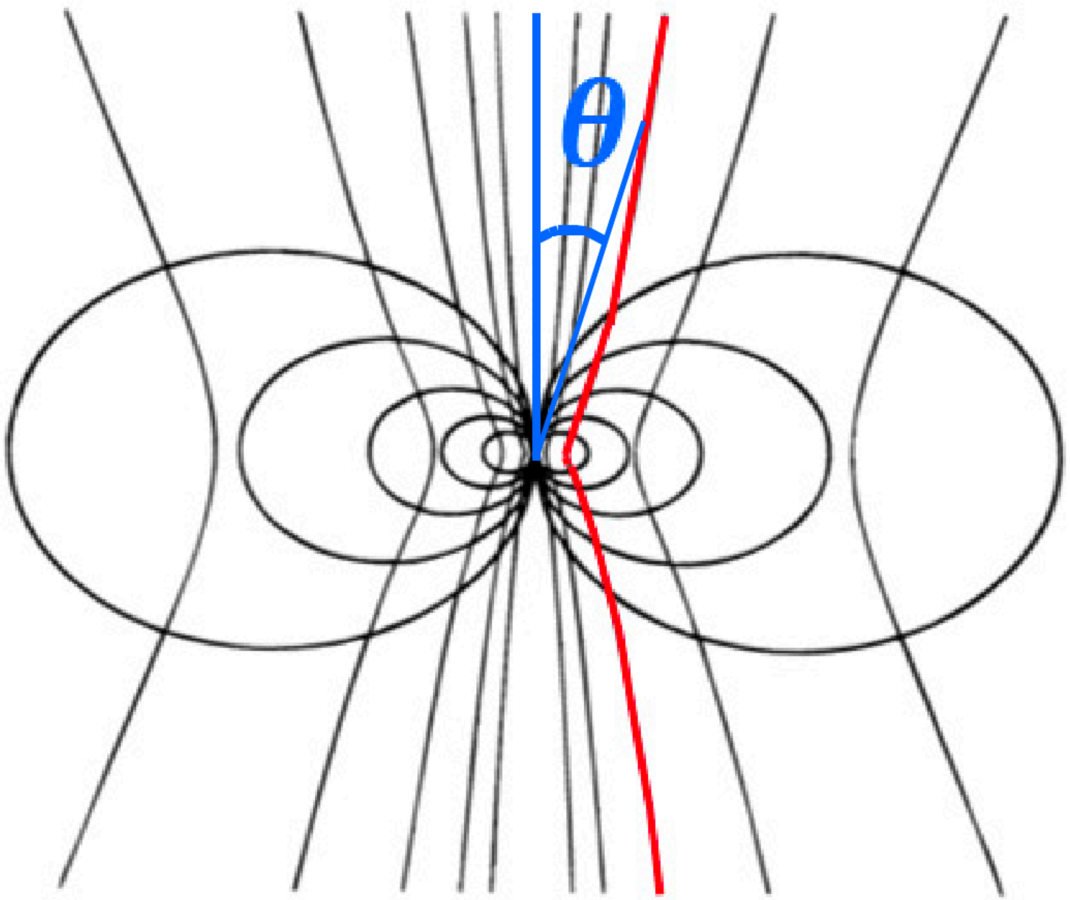

Padovani & Galli (2011)

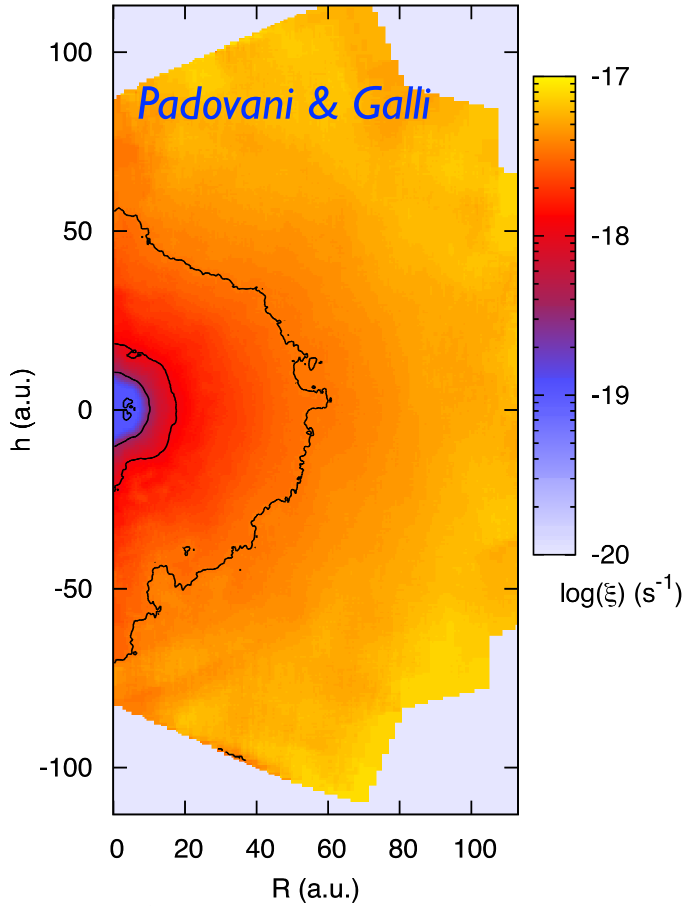

CR ionisation rate in the core interior

Equilibrium chemistry for non-ideal MHD: results

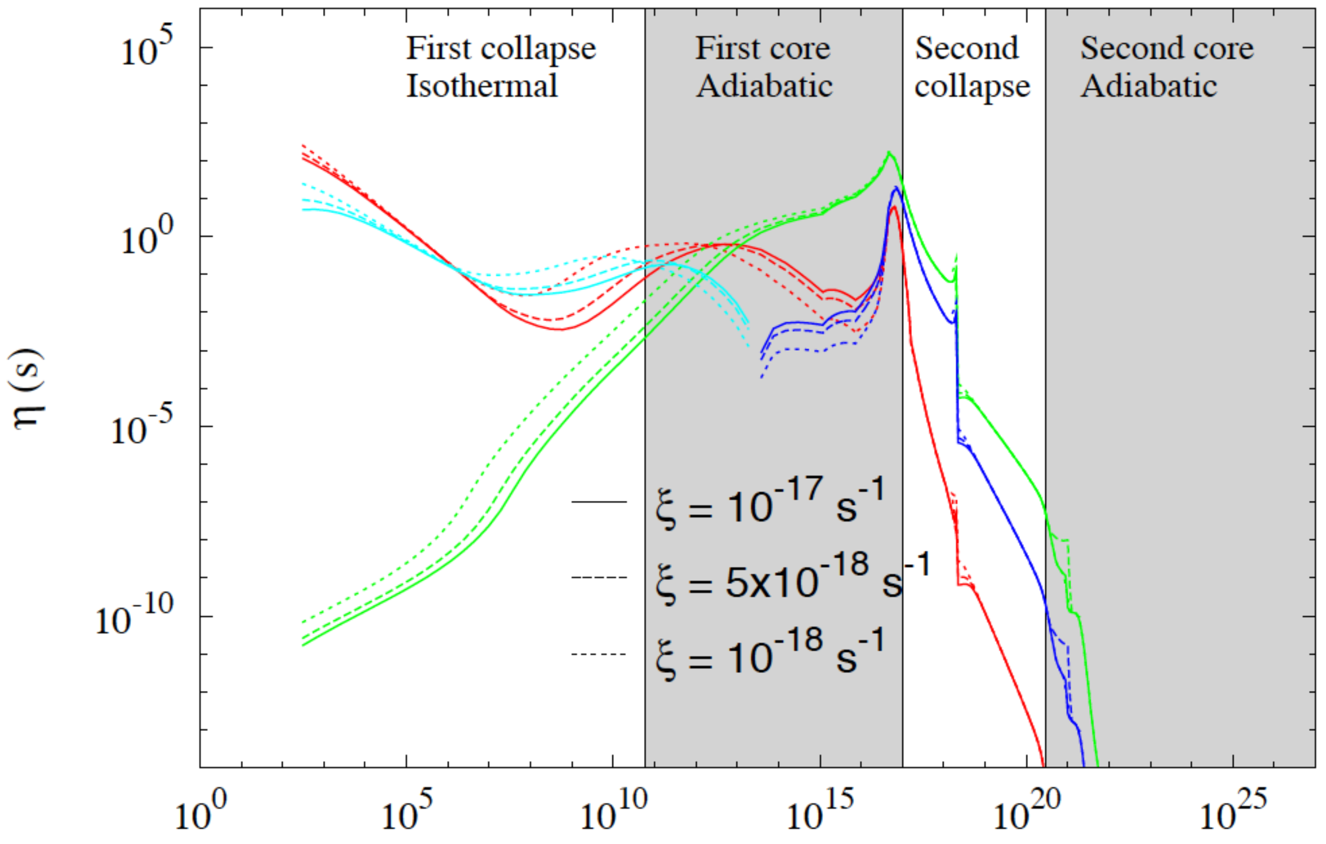

https://bitbucket.org/pmarchan/chemistry n_H (cm^{-3}) *Marchand et al. (2016)*

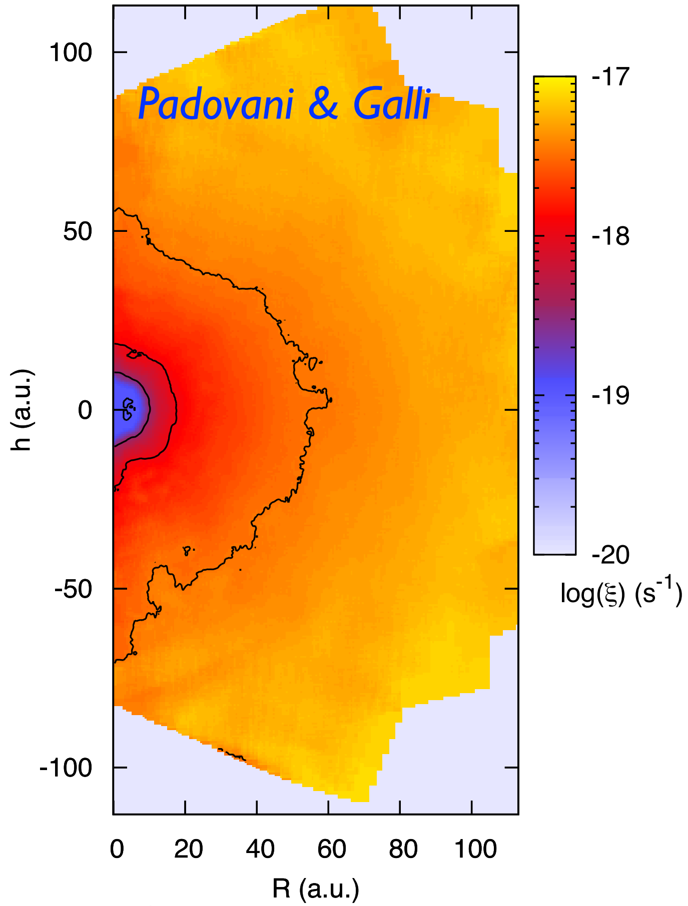

CR ionisation rate in the core interior

Standard numerical framework in 2020

- ✓ **Adaptive-mesh-refinement** code **RAMSES** (*Teyssier 2002*)
- ✓ **Non-ideal MHD** solver using Constrained Transport (*Teyssier et al. 2006, Fromang et al. 2006, Masson et al. 2012,2016*). Resistivity from steady-state gas-grain chemistry *(Marchand et al. 2016)*
- ✓ **Multifrequency Radiation-HD** solver using the Flux Limited Diffusion approximation *(Commerçon et al. 2011b, 2014, González et al. 2015)*. In most studies, just **grey**
- ✓ Other niMHD implementation: *Lesur et al. (2014)* in the **PLUTO** code, *Price et al. (2017)* in the SPH **Phantom** code, *Marinacci et al. (2018)* in the **AREPO** code

$$
\begin{aligned}
\partial_t \rho &+ \nabla \cdot [\rho \mathbf{u}] &&= 0 \\
\partial_t \rho \mathbf{u} &+ \nabla \cdot [\rho \mathbf{u} \otimes \mathbf{u} + P\mathbb{I}] &&= -\rho \nabla \Phi - \lambda \nabla E_\mathrm{r} + (\nabla \times \mathbf{B}) \times \mathbf{B} \\
\partial_t E_\mathrm{T} &+ \nabla \cdot [\mathbf{u}\,(E_\mathrm{T} + P_\mathrm{T}) - \mathbf{B}(\mathbf{B} \cdot \mathbf{u}) + \mathbf{E}_\mathrm{NIMHD} \times \mathbf{B}] &&= -\rho \mathbf{u} \cdot \nabla \Phi - \mathbb{P}_\mathrm{r} \nabla : \mathbf{u} - \lambda \mathbf{u} \nabla E_\mathrm{r} + \nabla \cdot \left(\frac{c\lambda}{\rho \kappa_\mathrm{R}} \nabla E_\mathrm{r} \right) \\
\partial_t E_\mathrm{r} &+ \nabla \cdot [\mathbf{u} E_\mathrm{r}] &&= -\mathbb{P}_\mathrm{r} \nabla : \mathbf{u} + \nabla \cdot \left(\frac{c\lambda}{\rho \kappa_\mathrm{R}} \nabla E_\mathrm{r} \right) + \kappa_\mathrm{P} \rho c (a_\mathrm{R} T^4 - E_\mathrm{r}) \\
\partial_t B &- \nabla \times (\mathbf{u} \times \mathbf{B}) - \nabla \times \mathbf{E}_\mathrm{NIMHD} &&= 0
\end{aligned}
$$

Resisitive EMF $\mathbf{E}_\mathrm{NIMHD} = +\eta_\Omega \mathbf{J} + \frac{\eta_\mathrm{H}}{||\mathbf{B}||} \mathbf{J} \times \mathbf{B} - \frac{\eta_\mathrm{AD}}{||\mathbf{B}||^2} \mathbf{J} \times \mathbf{B} \times \mathbf{B}$

1 M$_\odot$: Ambipolar diffusion

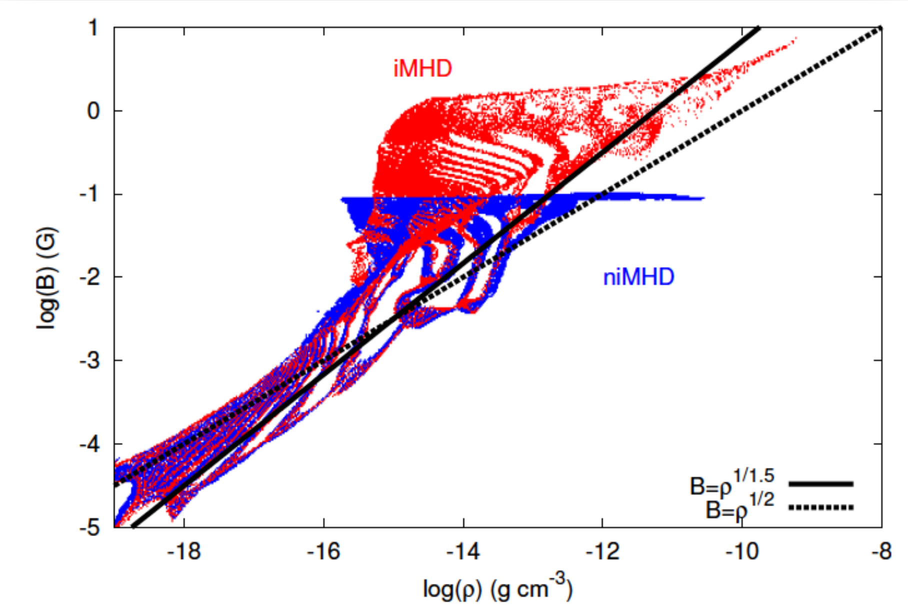

- formation of a **plateau** at B~0.1G
- **reorganisation** of magnetic field lines (essentially **poloidal**)

=> **reduced magnetic braking**

=> solution to the magnetic flux problem

Masson et al. (2016)

1 $M_\odot$: Ambipolar diffusion

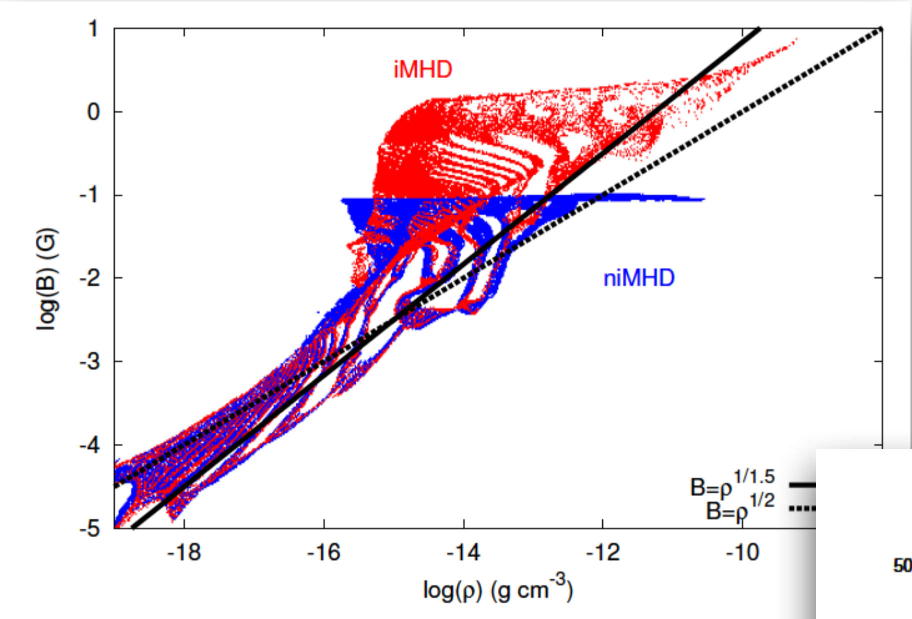

- formation of a **plateau** at B~0.1G
- **reorganisation** of magnetic field lines (essentially **poloidal**)

=> **reduced magnetic braking**

=> solution to the magnetic flux problem

- Rotationally supported disc formation (**R ~ 50 AU**) - consistent with obs.
- $P_{therm}/P_{mag}>1$ within discs
- **vertical** magnetic field in the disc

=> initial conditions for protoplanetary discs studies

Masson et al. (2016)

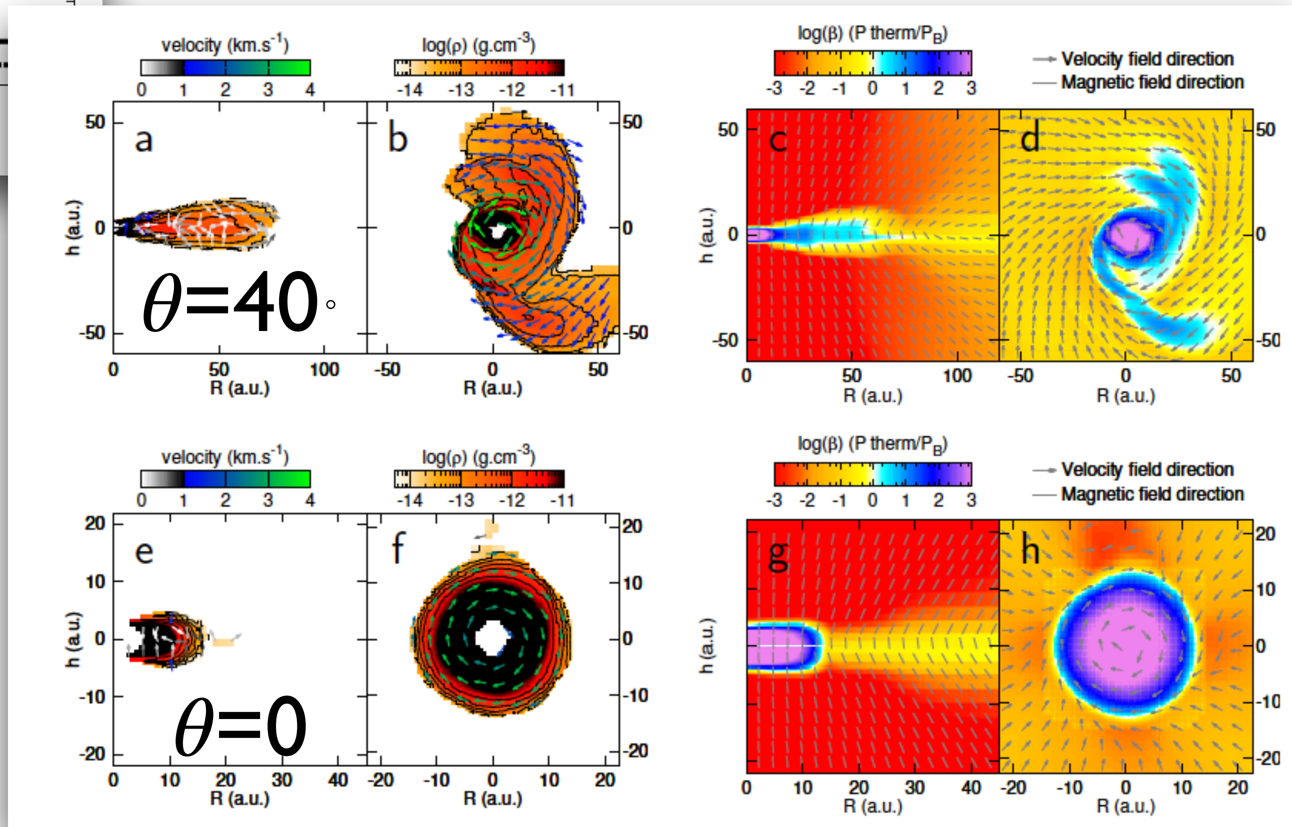

1 M⊙: Turbulence and ambipolar diffusion

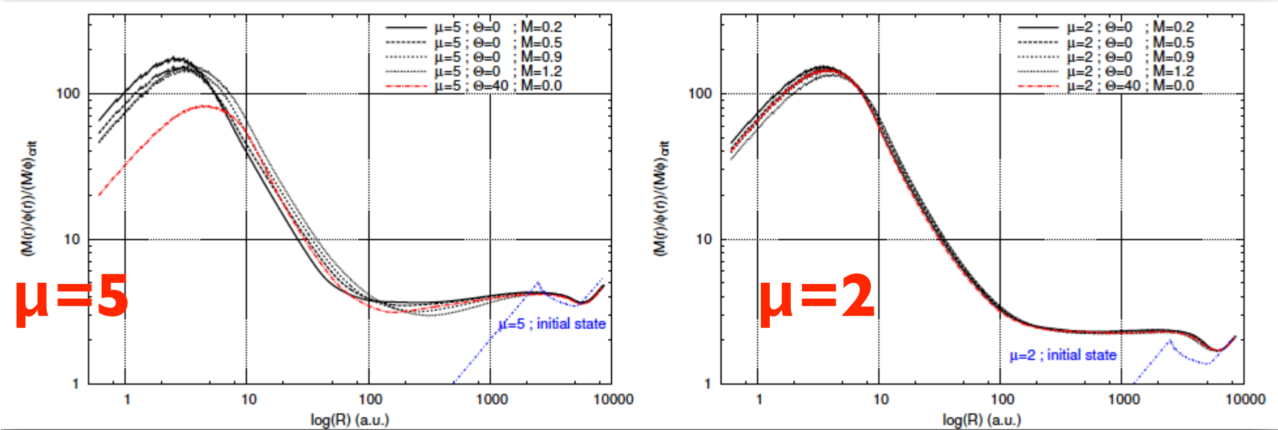

- magnetisation & disc size **does not depend** on turbulence level, nor on the initial magnetic field amplitude

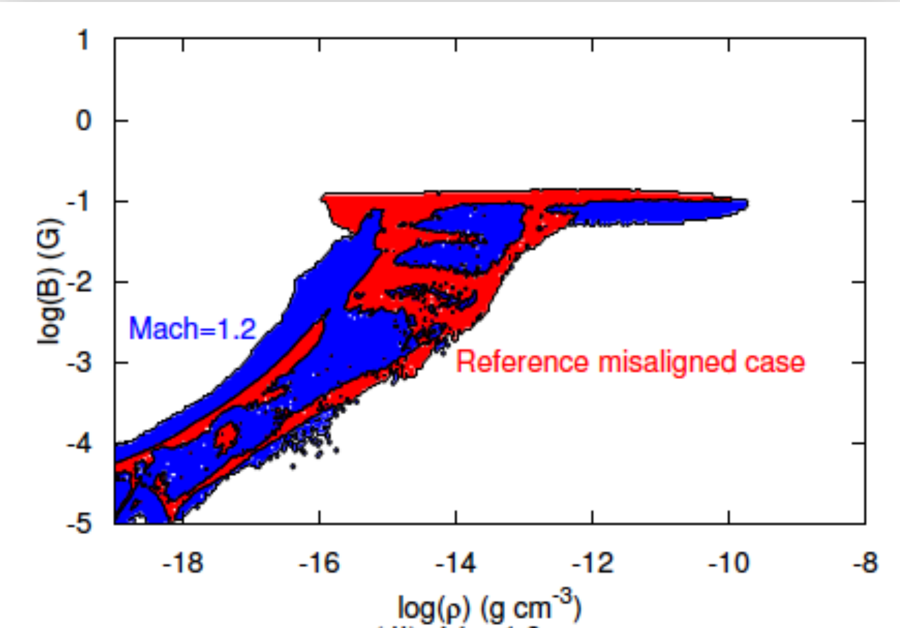

(.ii) $\mathcal{M} = 1.2$

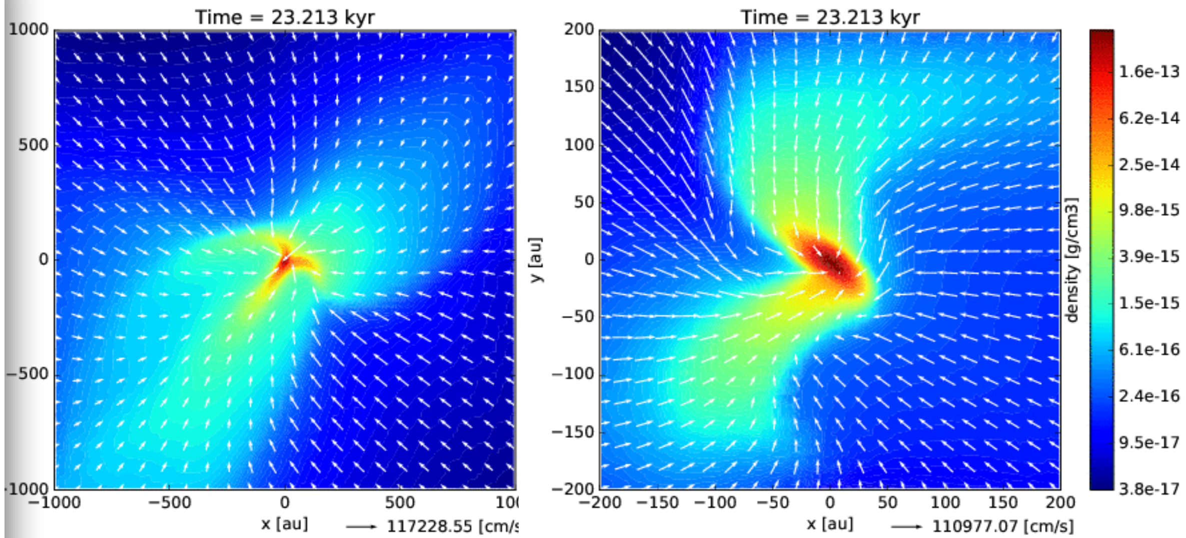

Convergence!

Long time integration

Low-mass core - 1M$_\odot$

100 kyr!

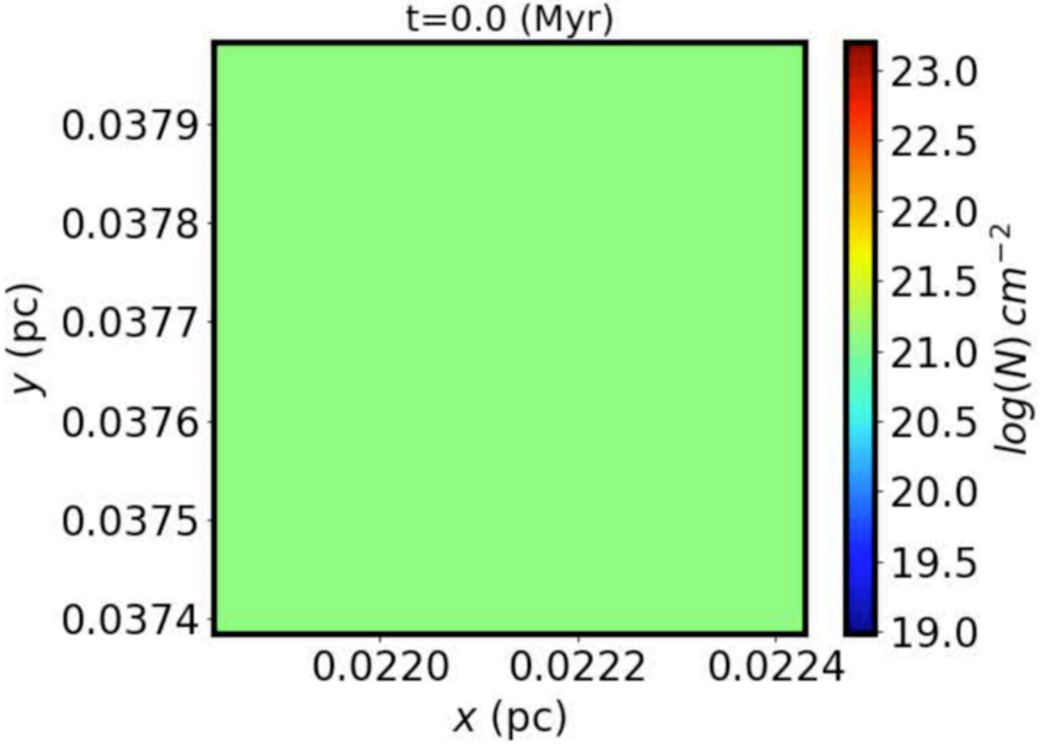

Hennebelle et al. (2020)

Massive core - 100 M$_\odot$

70 kyr

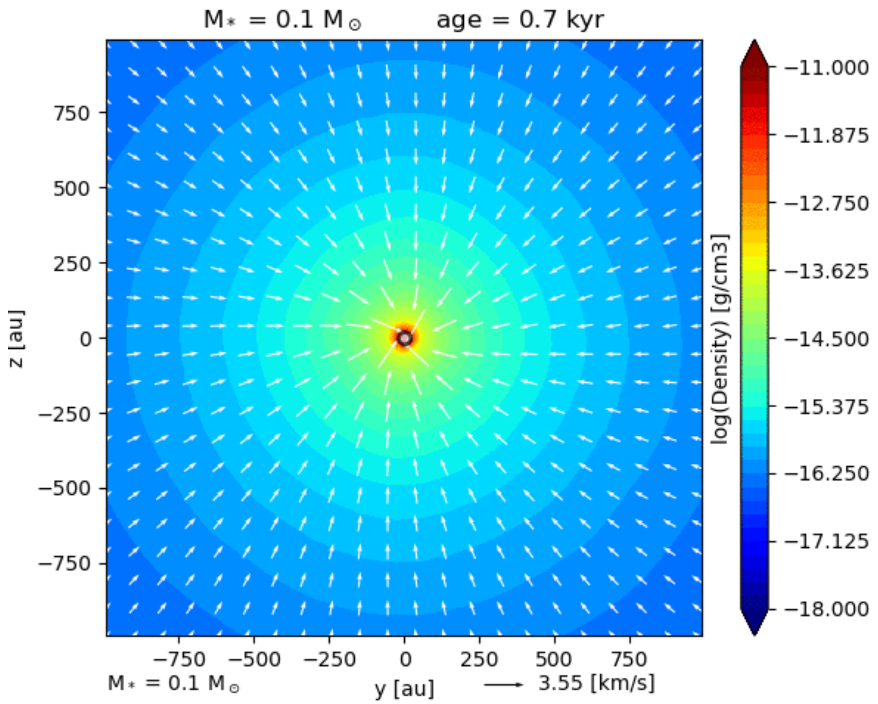

Commerçon et al. (2021)

Magnetically regulated disc size with AD

Hennebelle et al. (2016)

$$\tau_{\rm far} \simeq \frac{B_\phi h}{B_z v_\phi} \qquad \tau_{\rm br} \simeq \frac{\rho v_\phi 4\pi h}{B_z B_\phi}$$

$$\tau_{\rm diff} \simeq \frac{4\pi h^2}{c^2 \eta_{\rm AD}} \frac{B_z^2 + B_\phi^2}{B_z^2} \simeq \frac{4\pi h^2}{c^2 \eta_{\rm AD}} \qquad \tau_{\rm rot} \simeq \frac{2\pi r}{v_\phi}$$

$$r_{\rm d,AD} \simeq 18 \text{ au} \times \delta^{2/9} \left(\frac{\eta_{\rm AD}}{0.1 \text{ s}}\right)^{2/9} \left(\frac{B_z}{0.1 \text{ G}}\right)^{-4/9} \left(\frac{M_{\rm d} + M_*}{0.1\, M_\odot}\right)^{1/3}$$

- disc size **does not depend** on turbulence level
- weak dependance on the mass

vs.

$$r_{\rm d,hydro} \simeq \frac{\Omega_0^2 R_0^4}{4\pi/3 \rho_0 R_0^3 G} = 3\beta R_0 = 106 \text{ AU} \, \frac{\beta}{0.02} \left(\frac{M}{0.1\,{\rm M}_\odot}\right)^{1/3} \left(\frac{\rho_0}{10^{-18} {\rm g\,cm}^{-3}}\right)^{-1/3}$$

Magnetically regulated disc size with AD

$$r_{\mathrm{d,AD}} \simeq 18\ \mathrm{au} \times \delta^{2/9} \left(\frac{\eta_{\mathrm{AD}}}{0.1\ \mathrm{s}}\right)^{2/9} \left(\frac{B_z}{0.1\ \mathrm{G}}\right)^{-4/9} \left(\frac{M_{\mathrm{d}} + M_*}{0.1\ M_\odot}\right)^{1/3}$$

Hennebelle et al. (2016)

- very good agreement between the analytical and experimental values
- disc size **does not depend** (too much) **on initial conditions**

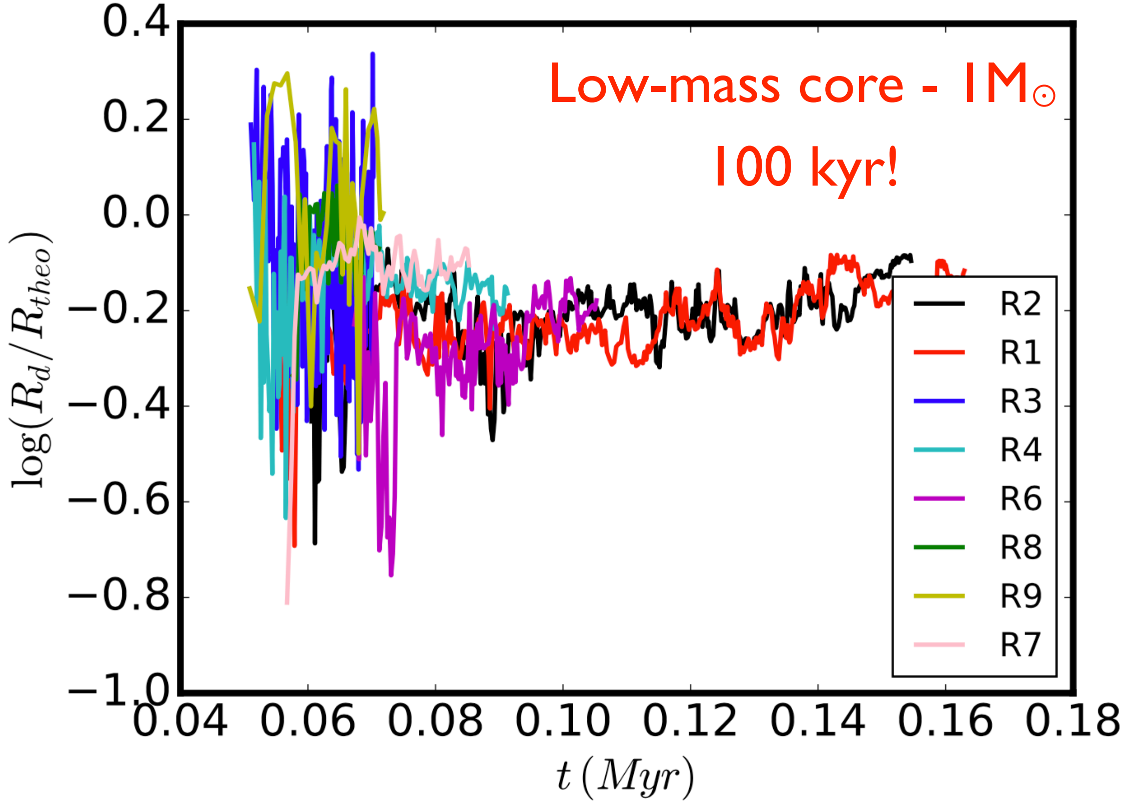

Hennebelle et al. (2020)

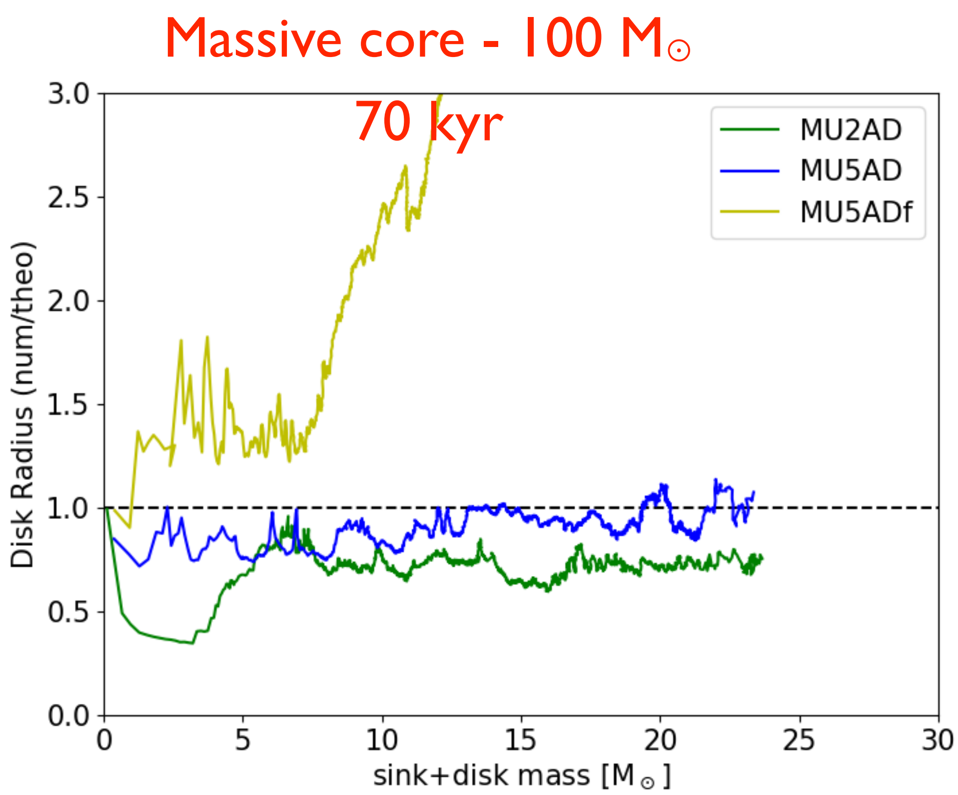

Commerçon et al. (2021)

Take away II

✓ Disc formation is regulated by non-ideal processes

✓ Magnetic regulation works for low- and high-mass protostar formation

✓ Prediction of magnetic fields properties at disc (au) scales

Outline

1. Introduction
2. Dense core collapse, disc formation (pc to au)
3. **Formation of the protostar (au to $R_\odot$)**
4. Observations
5. Perspectives

Star formation evolutionary sequence

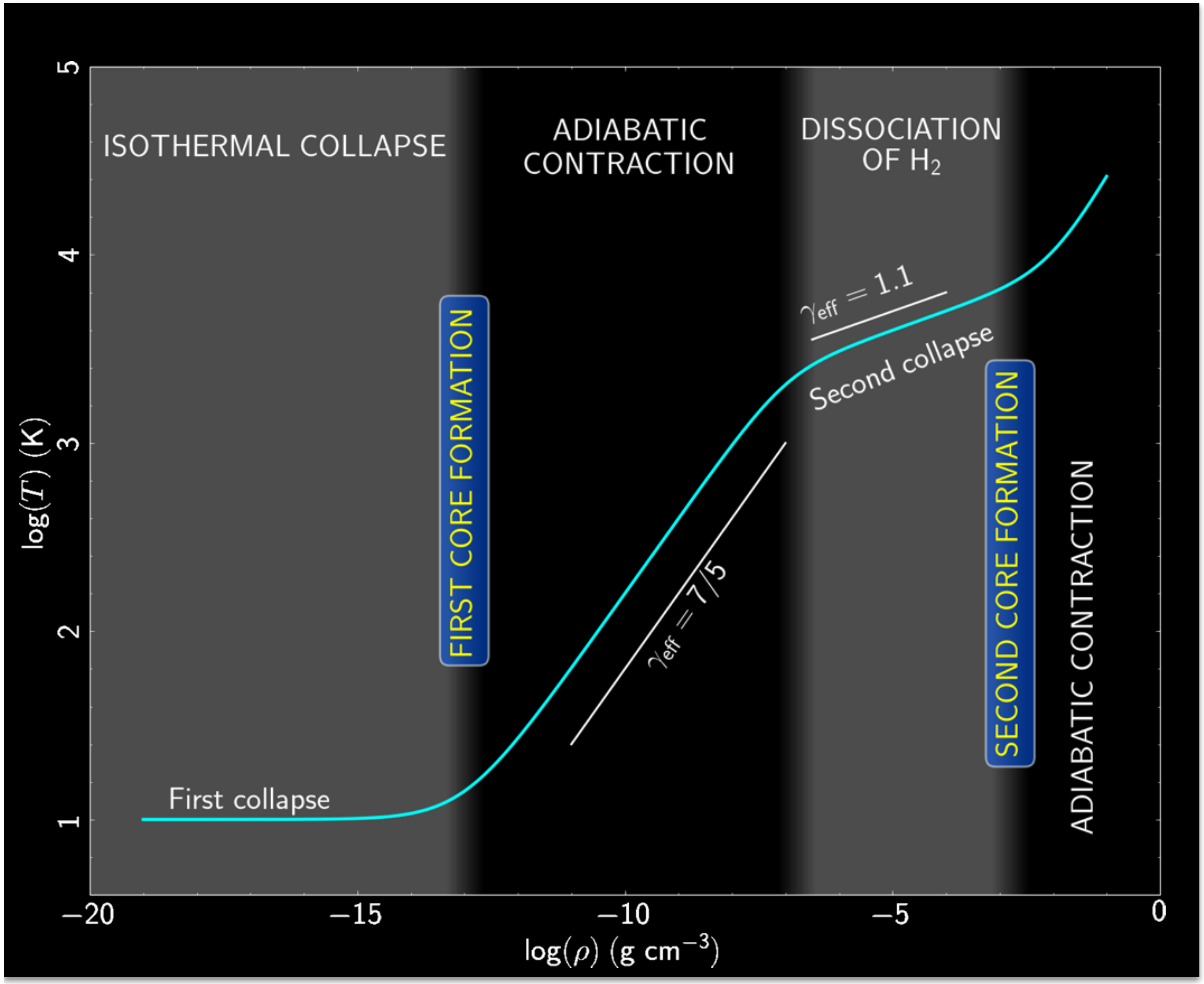

Vaytet et al. (2013)

$$M_{\rm Jeans} \propto \rho^{3\gamma_{\rm eff}-4}$$

Prestellar dense core collapse
(R=0.01 pc, T=10 K, n=10^6 cm^{-3})

First collapse

Isothermal ↓ ***$10^{4,5}$ yr***

First Larson core
(R=10 AU, T=100 K, n=10^{12} cm^{-3})

Adiabatic ↓ ***a few 10^3 yr***

H_2 dissociation

Second collapse

Quasi - isothermal ↓ ***10^2 yr***

Second Larson core
(R=0.01 AU, T=10^{4-5} K, n=0.01cm^{-3})

Larson (1969)

Second collapse

- Ohmic + ambipolar diffusion
- non-ideal gas EOS

Vaytet et al. (2018)

Saumon, Chabrier & Von Horn (1995)

- maximum resolution : $\Delta x \sim 8 \times 10^{-5}$ AU (21 AMR levels)

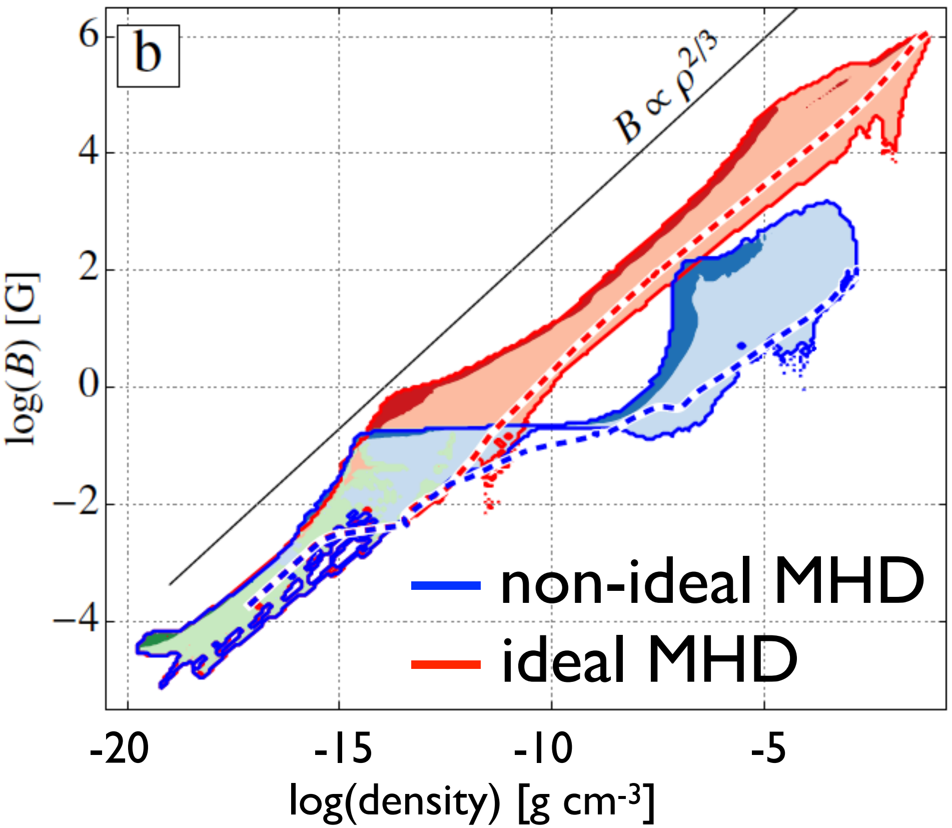

Magnetic flux reduced by ~3 orders of magnitude with **ambipolar diffusion** and **Ohmic diffusion**

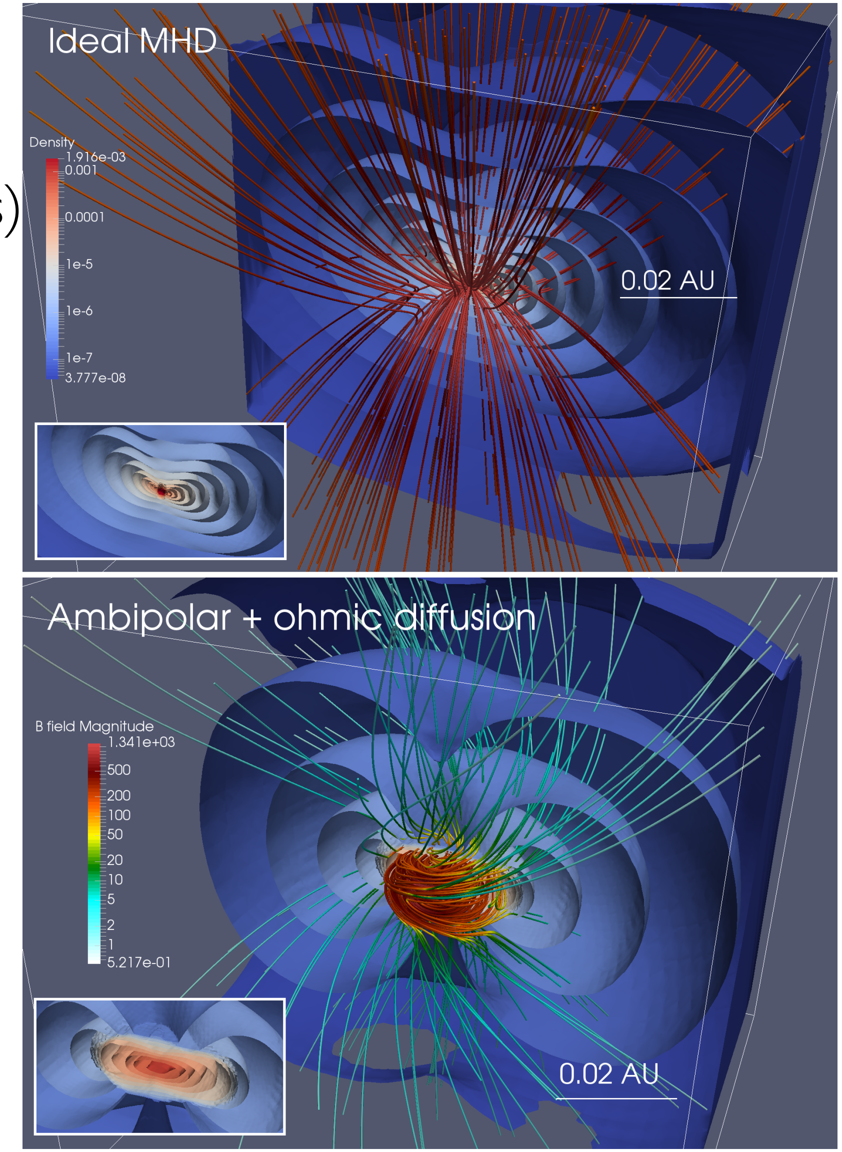

See *also* *Wurster et al. (2018)*

Second collapse

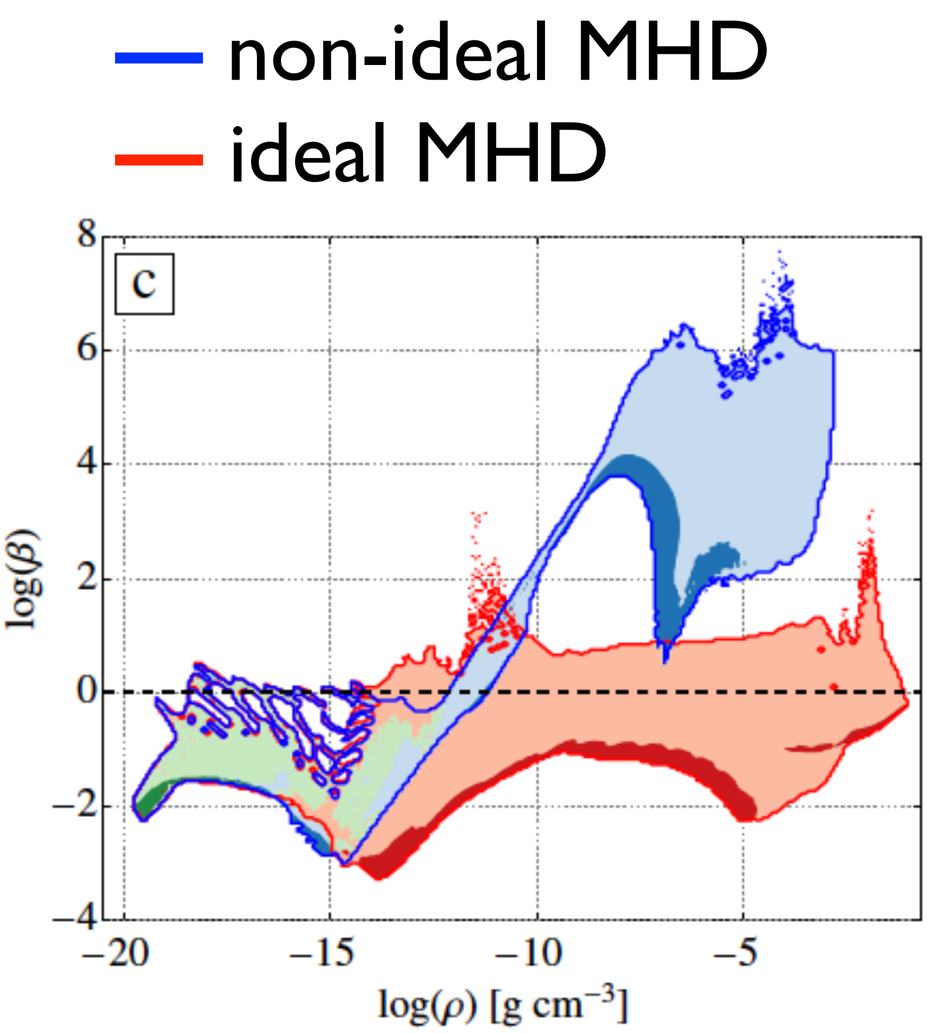

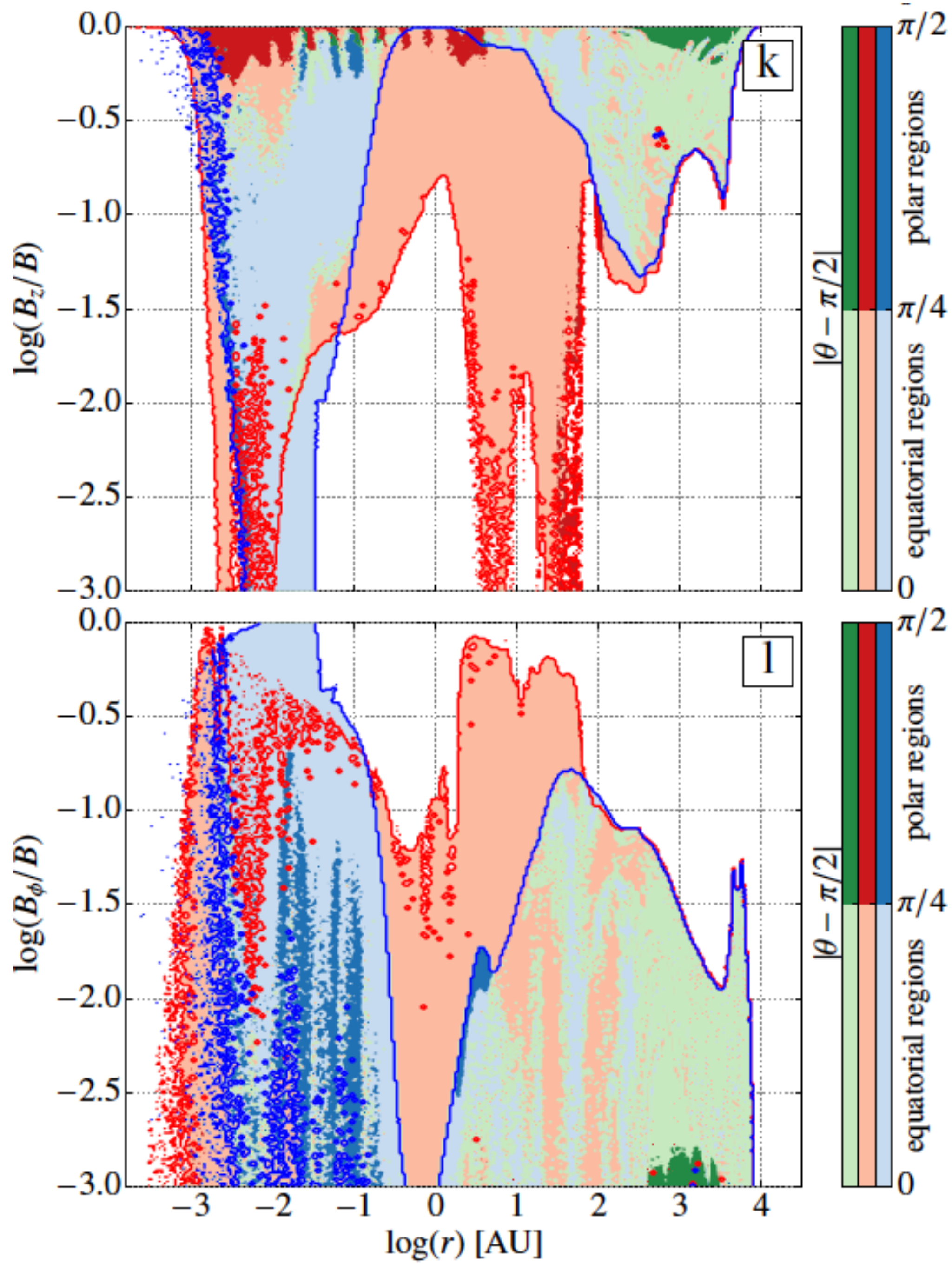

Vaytet et al. (2018)

Disc birth

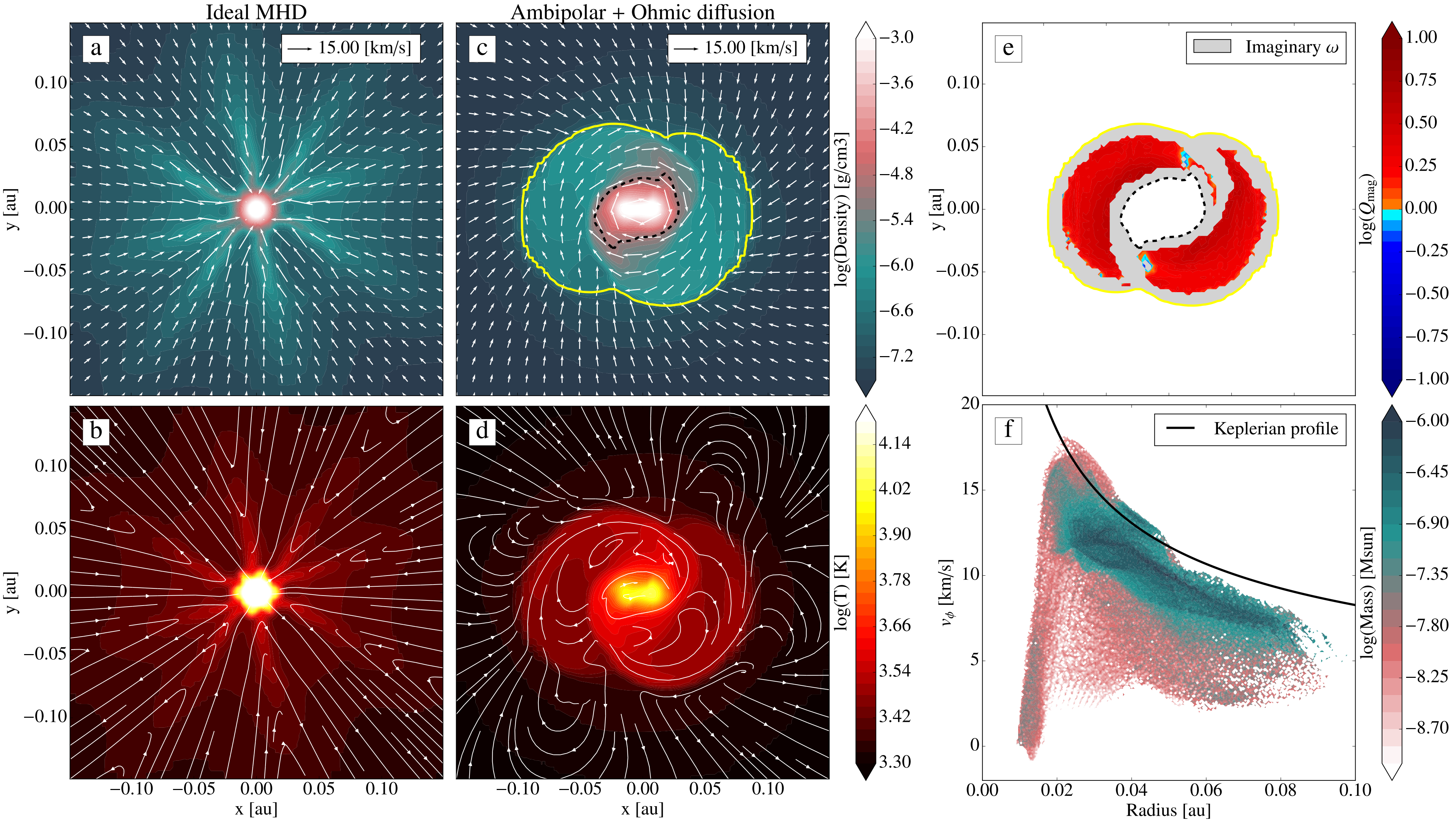

Vaytet et al. (2018)

Radiative shocks

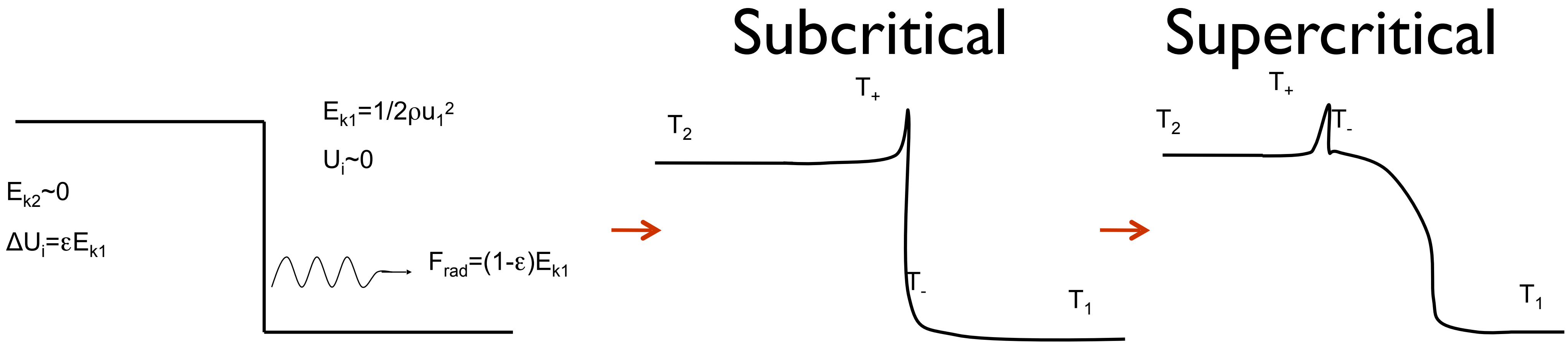

- Jump conditions (Rankine-Hugoniot)

$$\rho_1 u_1 = \rho_2 u_2 \equiv \dot{m},$$
$$\rho_1 u_1^2 + P_1 + P_{r1} = \rho_2 u_2^2 + P_2 + P_{r2},$$
$$\dot{m}\left(h_1 + \rho_1 u_1^2\right) + F_{r1} + u_1\left(E_{r1} + P_{r1}\right) =$$
$$\dot{m}\left(h_2 + \rho_2 u_2^2\right) + F_{r2} + u_2\left(E_{r2} + P_{r2}\right)$$

- Shock becomes supercritical if $T_- > T_{cr}$

$$T_{cr} = \left(\frac{u_1 \rho_1 k_B}{(\gamma - 1)\mu m_H \sigma}\right)^{1/3}$$

Properties of the radiative accretion shock

Vaytet et al. (2018)

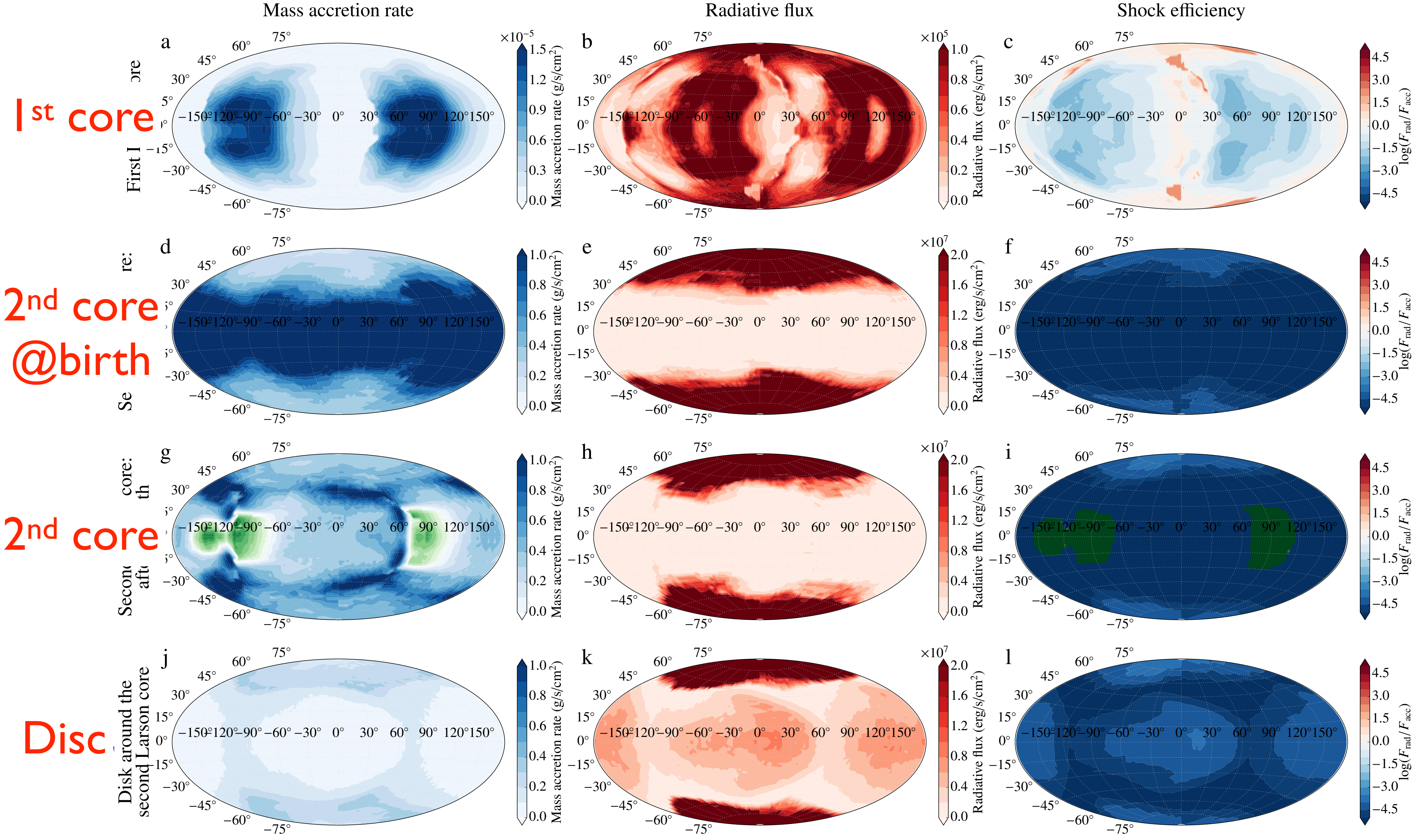

Early evolution of the second core

Bhandare et al. (2020)

Parametric study based on the initial dense core mass (0.5 to 100 $M_\odot$) using PLUTO with non-ideal gas EOS and radiative transport (FLD)

But…

- Need to lower the dimensionality => 2D axisymmetric models
- No initial rotation, no magnetic fields
- Integration up to 400 years

Early evolution of the second core

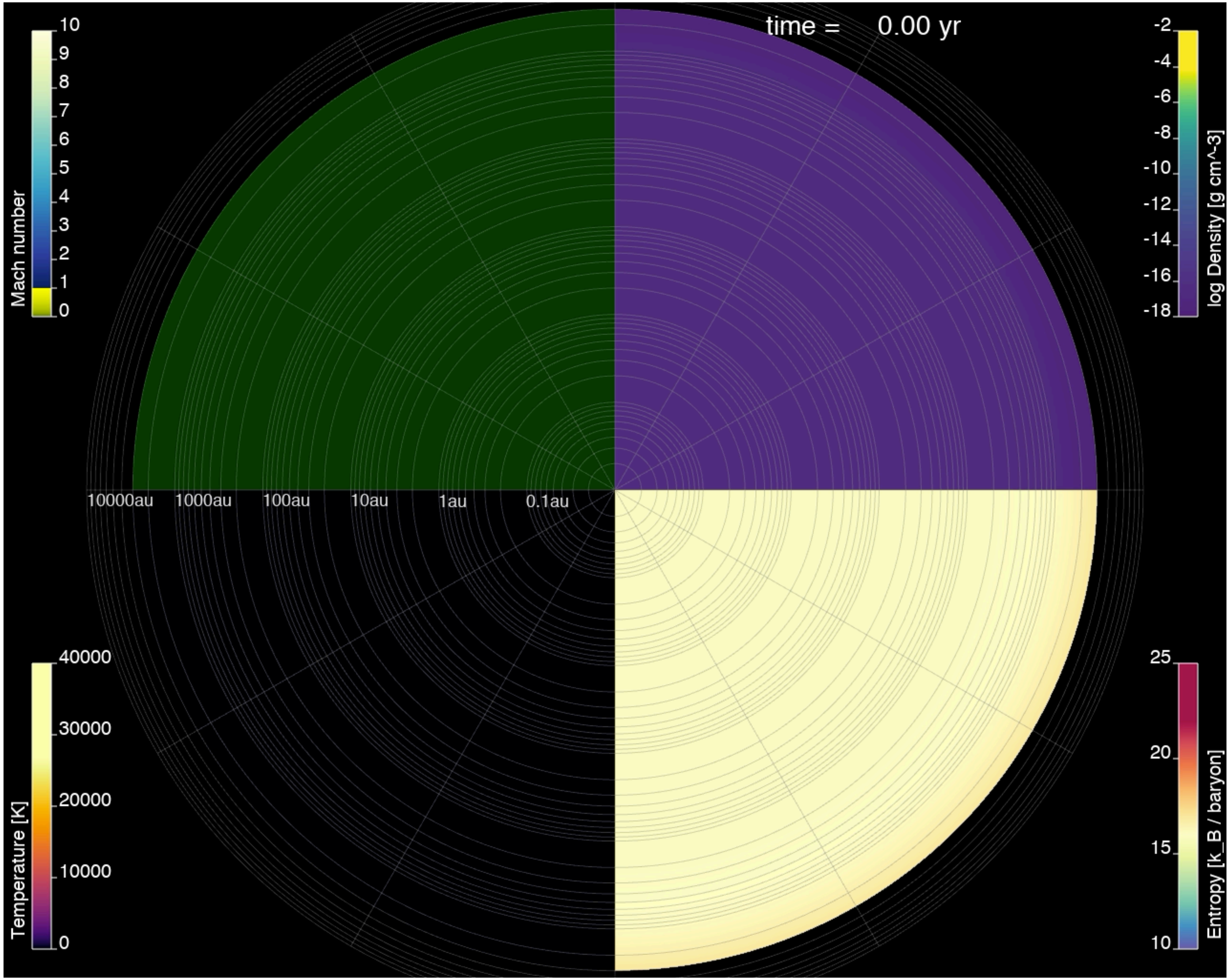

Bhandare et al. (2020)

Early evolution of the second core

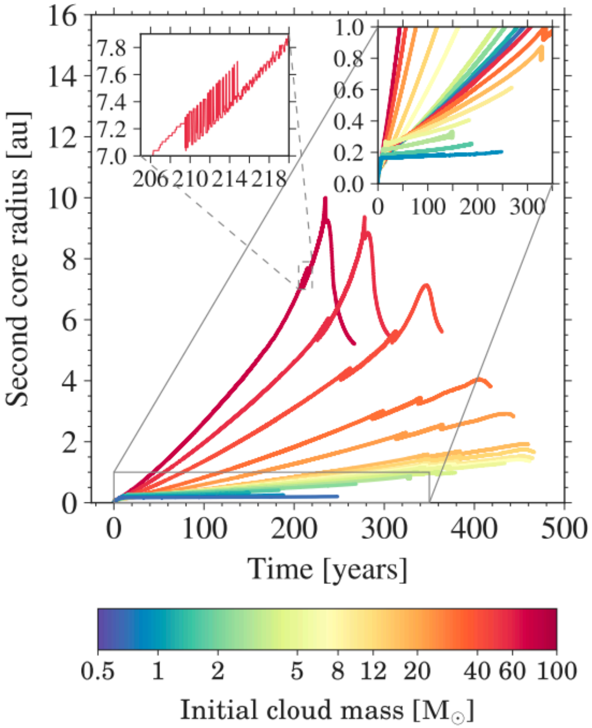

- Second core expansion (faster when mass increases)
- Development of convective eddies

=> Quid of magnetic fields? Effect of rotation?

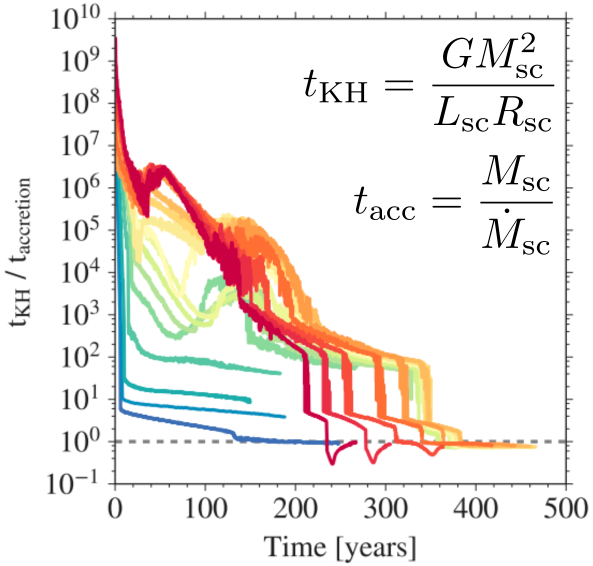

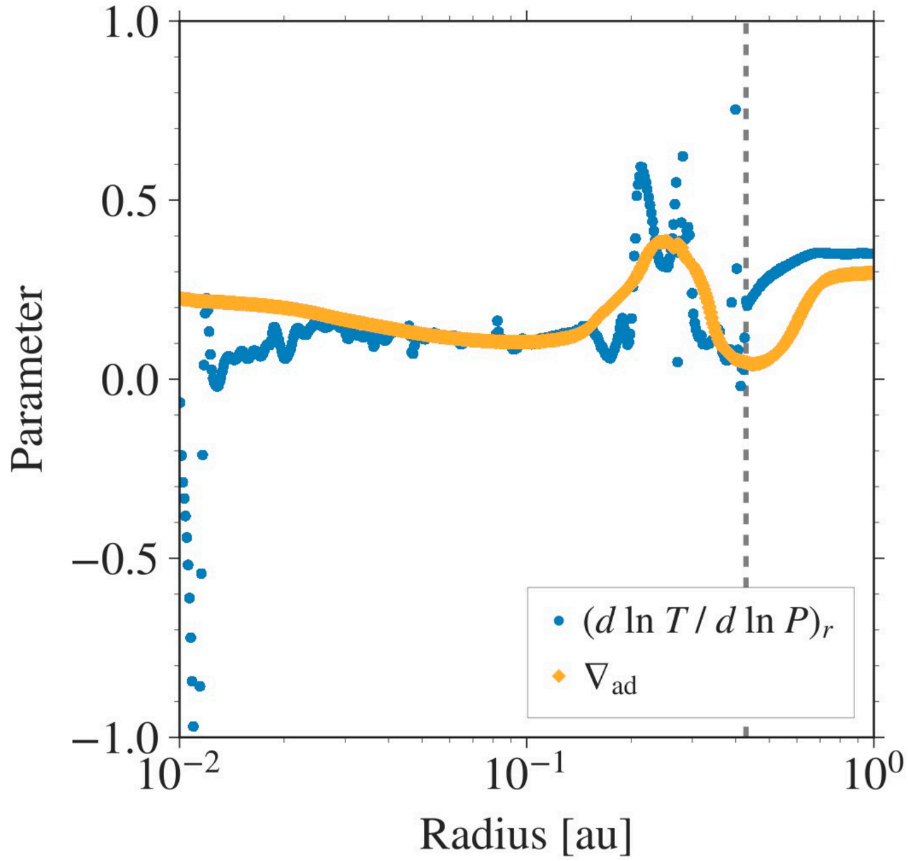

Bhandare et al. (2020)

Take away III

- ✓ Disc and protostar formation and early evolution highly dependent on the physics included
- ✓ Angular momentum and magnetic flux problems have a solution
- ✓ Non ideal MHD is required
- ✓ Early convection is plausible
- ✓ Robustness of the predictions of magnetic properties in class 0 protostars?

Next:

- Longer term evolution
- Consider the environment of dense core (late accretion, streamers)
- Parametric studies of 2nd collapse

What about observations?

Orion Class 0 - ALMA

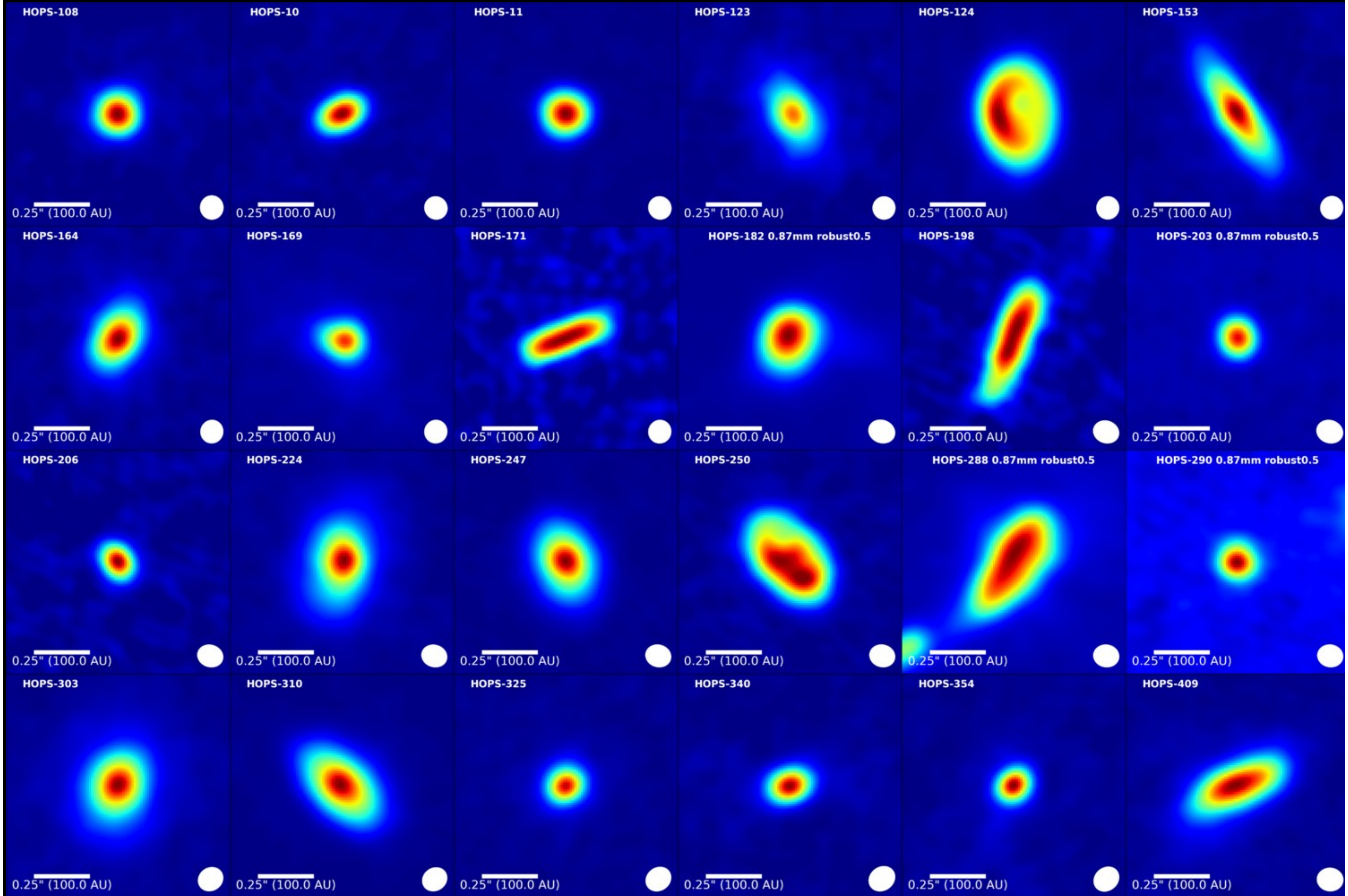

Credits: John Tobin - VANDAM survey

Disc radius

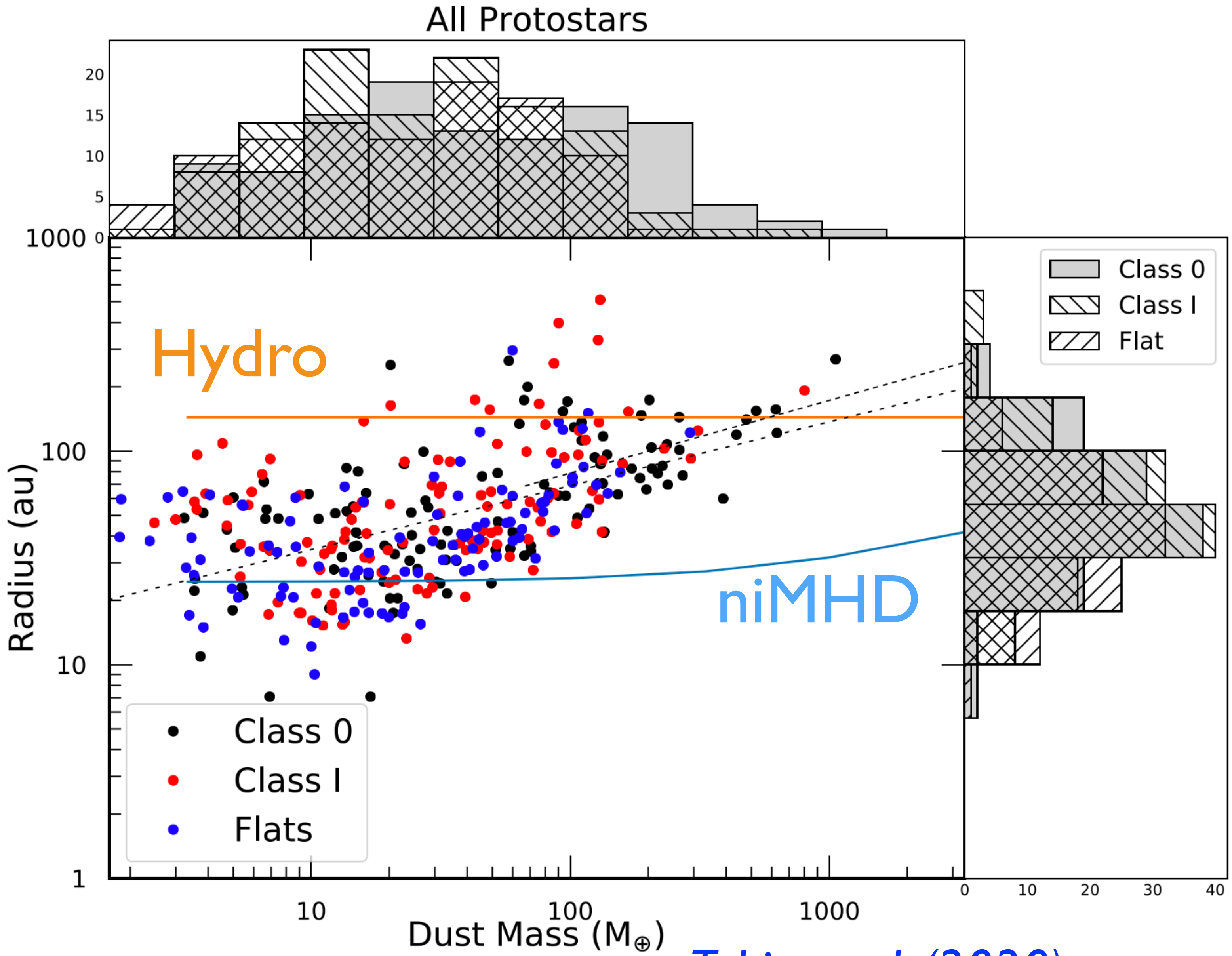

Tobin et al. (2020)
VANDAM survey

Magnetically regulated collapse?

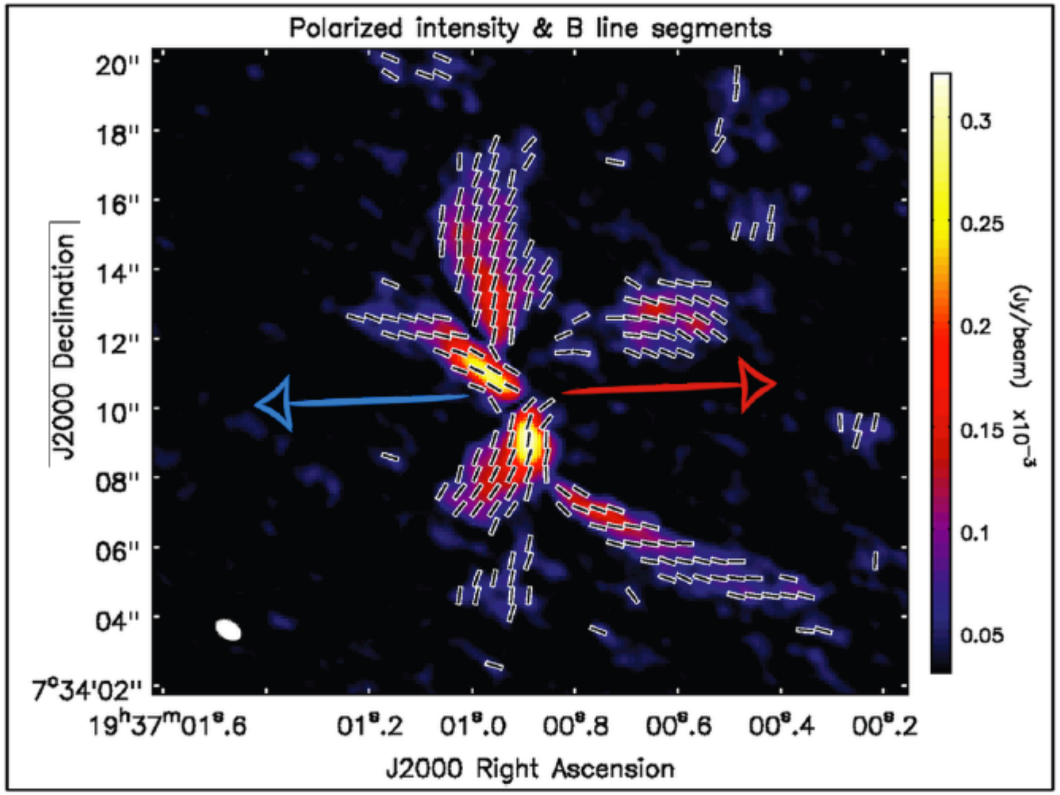

Maury et al. (2018)

B335 Class 0

- ALMA 0.8'' @ 233 GHz (~60 AU)
- data "consistent" with magnetised collapse model (2.5M$_\odot$; μ=6 ; low rotation)

- *Yen et al. (2015)*: No Keplerian disc with R>10 AU
=> Magnetic braking or young age?
- *Yen et al. (2018)*: No evidence of ion-neutral decoupling at scales > 100 AU ($HCO^+/C^{18}O$)

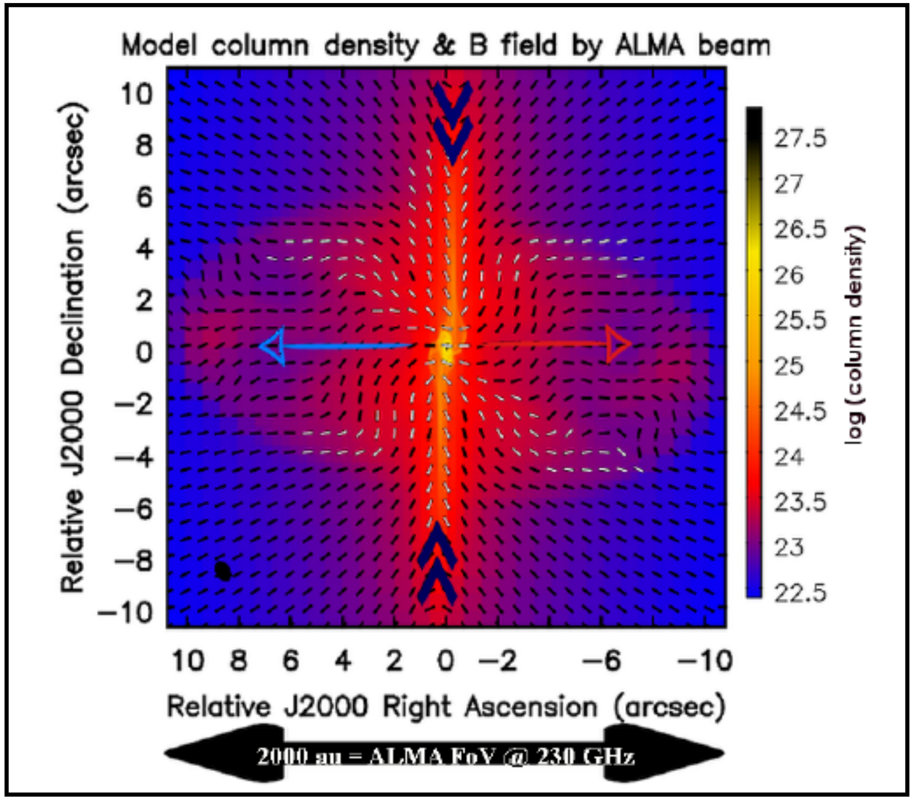

Disc radius evolution

Tychoniec et al. (2020)

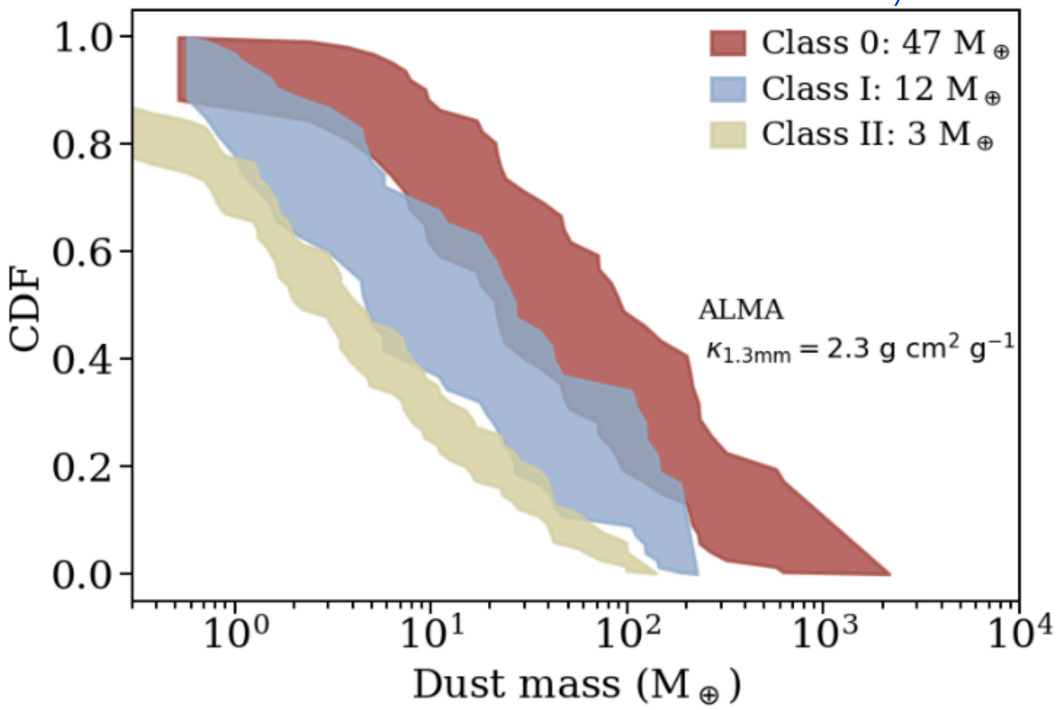

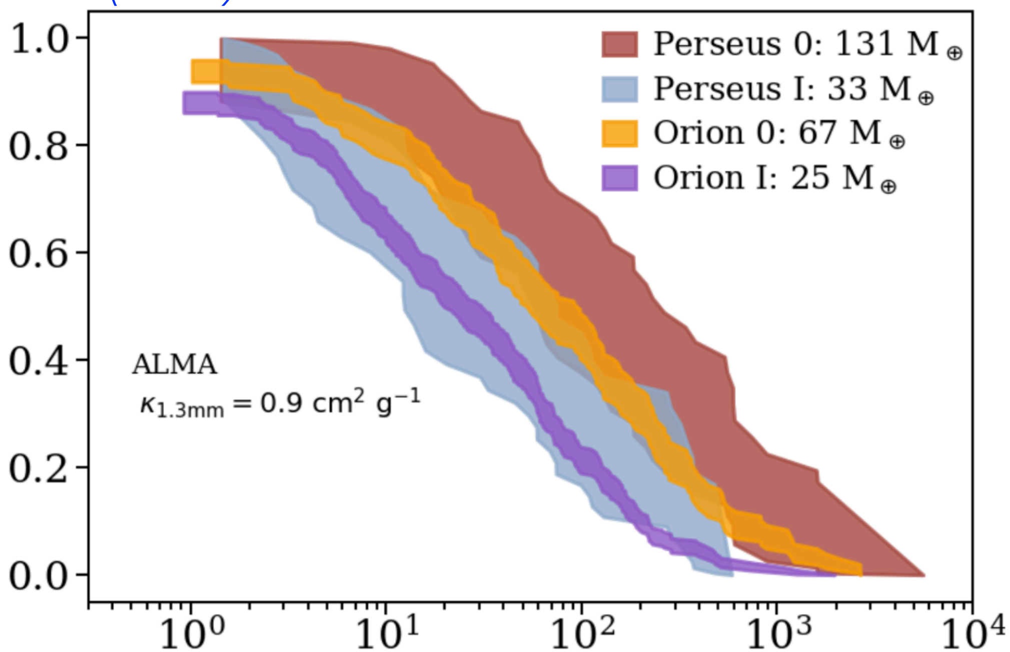

Disc mass decreases with time
Disc radius increases with time
Disc size compatible with niMHD
(Lebreuilly+21)

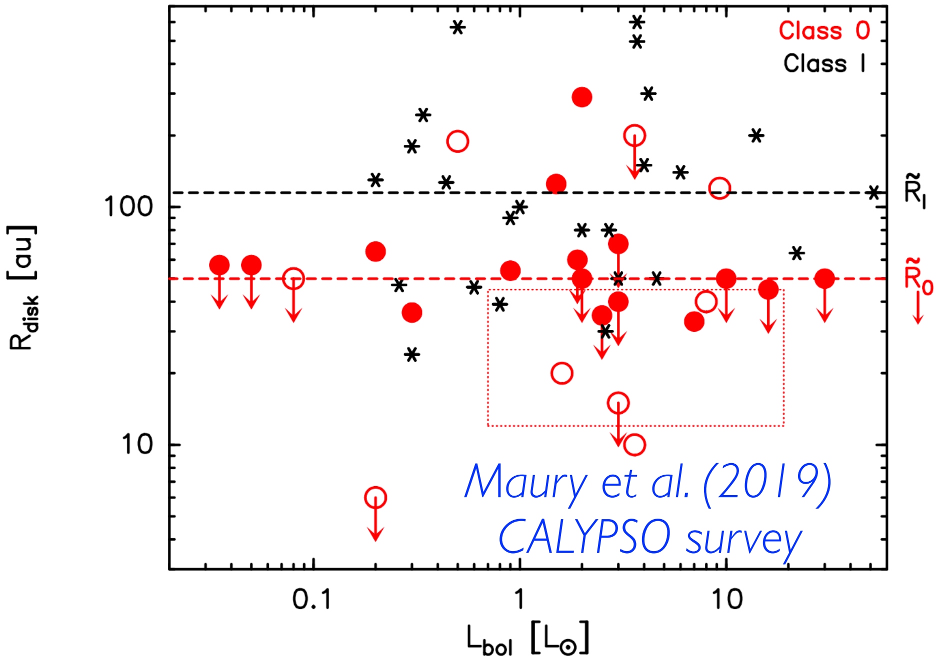

Evidences of dust evolution

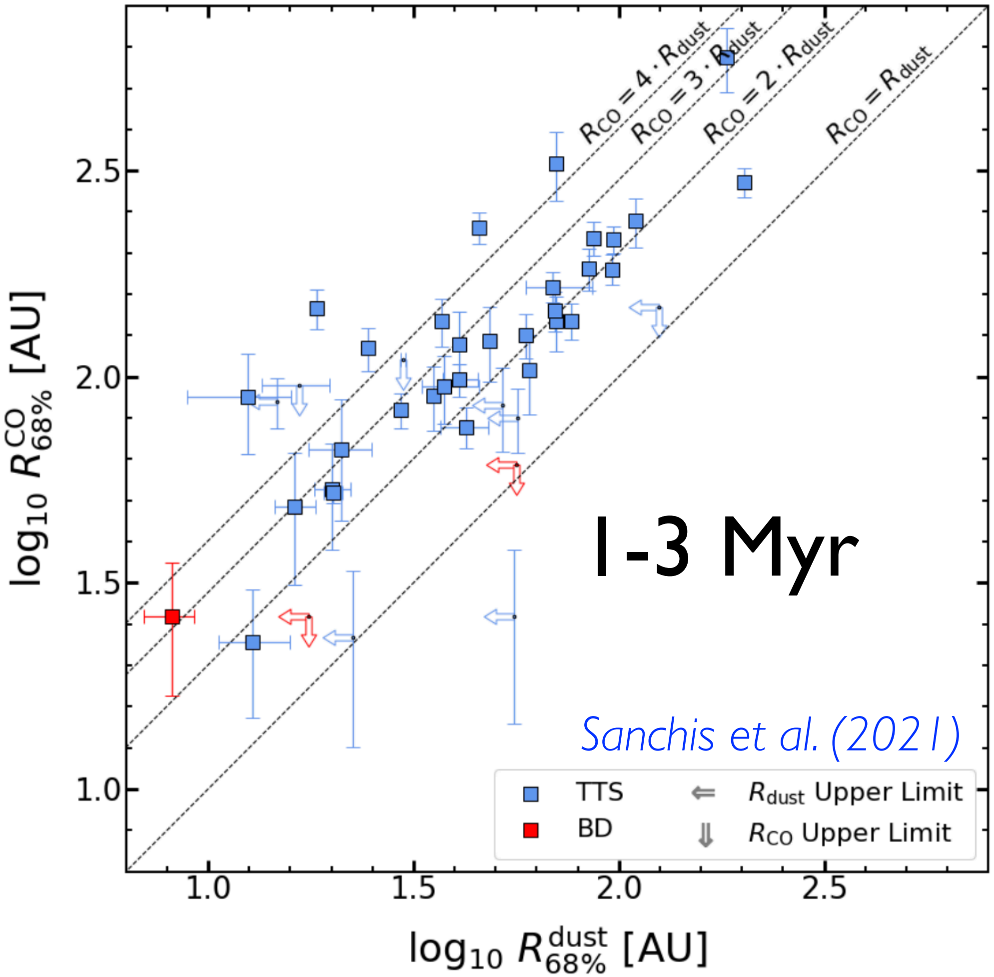

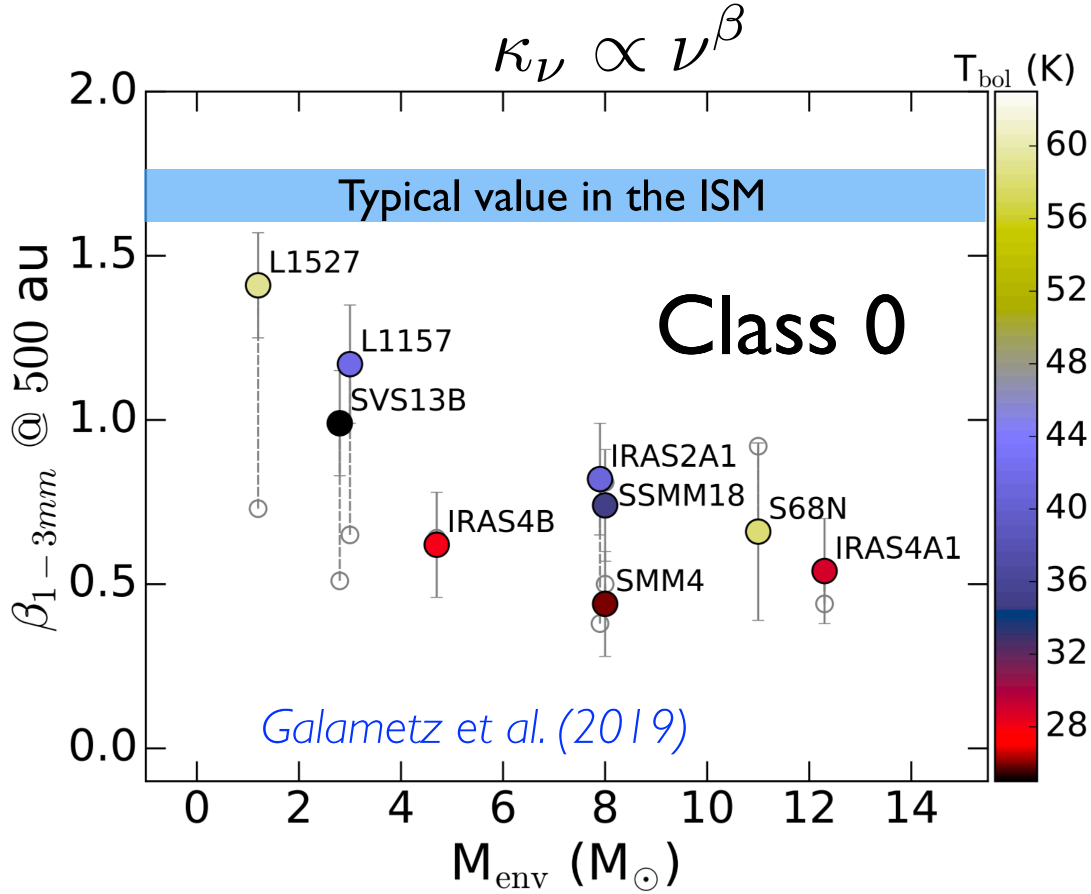

- Gas disc is 2-3 times larger than the dust discs
- Discs are enriched in dust compared to the ISM
- Evidence of large grains

Dust grains drift and grow!

Gas-dust dynamical coupling

Drag force

$$\mathbf{F}_{\mathrm{g/d}} = -\frac{m_{\mathrm{grain}}}{t_{\mathrm{s}}}(\mathbf{v}_{\mathrm{d}} - \mathbf{v}_{\mathrm{g}})$$

Stopping time (Epstein 1924)

$$t_{\mathrm{s}} = \sqrt{\frac{\pi\gamma}{8}}\frac{\rho_{\mathrm{grain}}}{\rho}\frac{s_{\mathrm{grain}}}{c_{\mathrm{s}}}$$

Coupling with the gas (Stokes number)

$$\mathrm{St} \equiv \frac{t_{\mathrm{s}}}{t_{\mathrm{dyn}}}$$

- If St<1, strong coupling
- If St>1, poor coupling

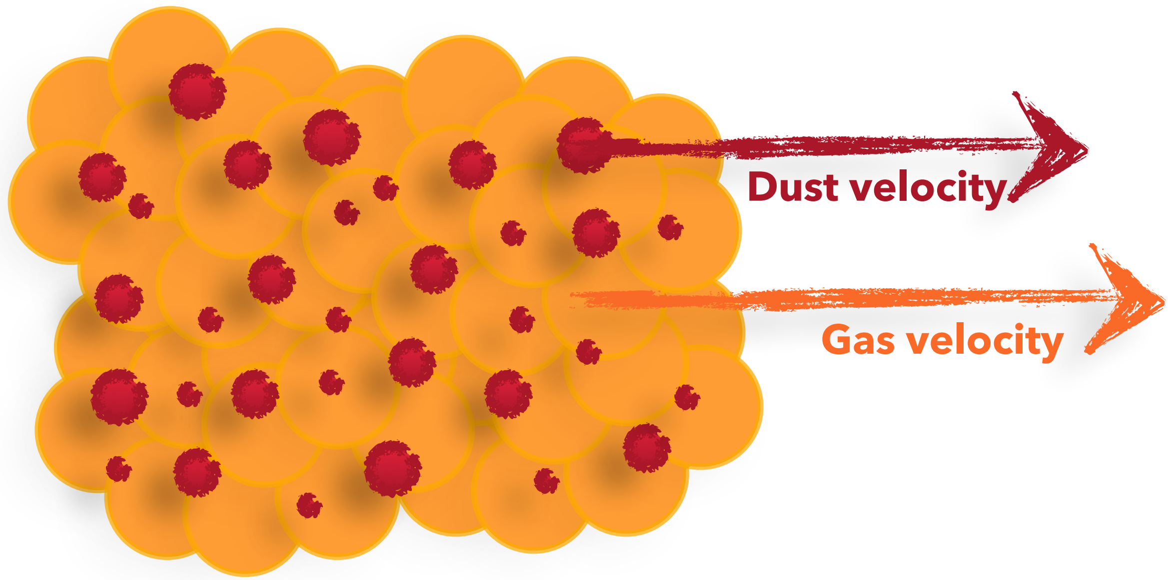

Lebreuilly et al. (2019, 2020)

Dust in RAMSES

Collapse with dust and gas dynamical coupling

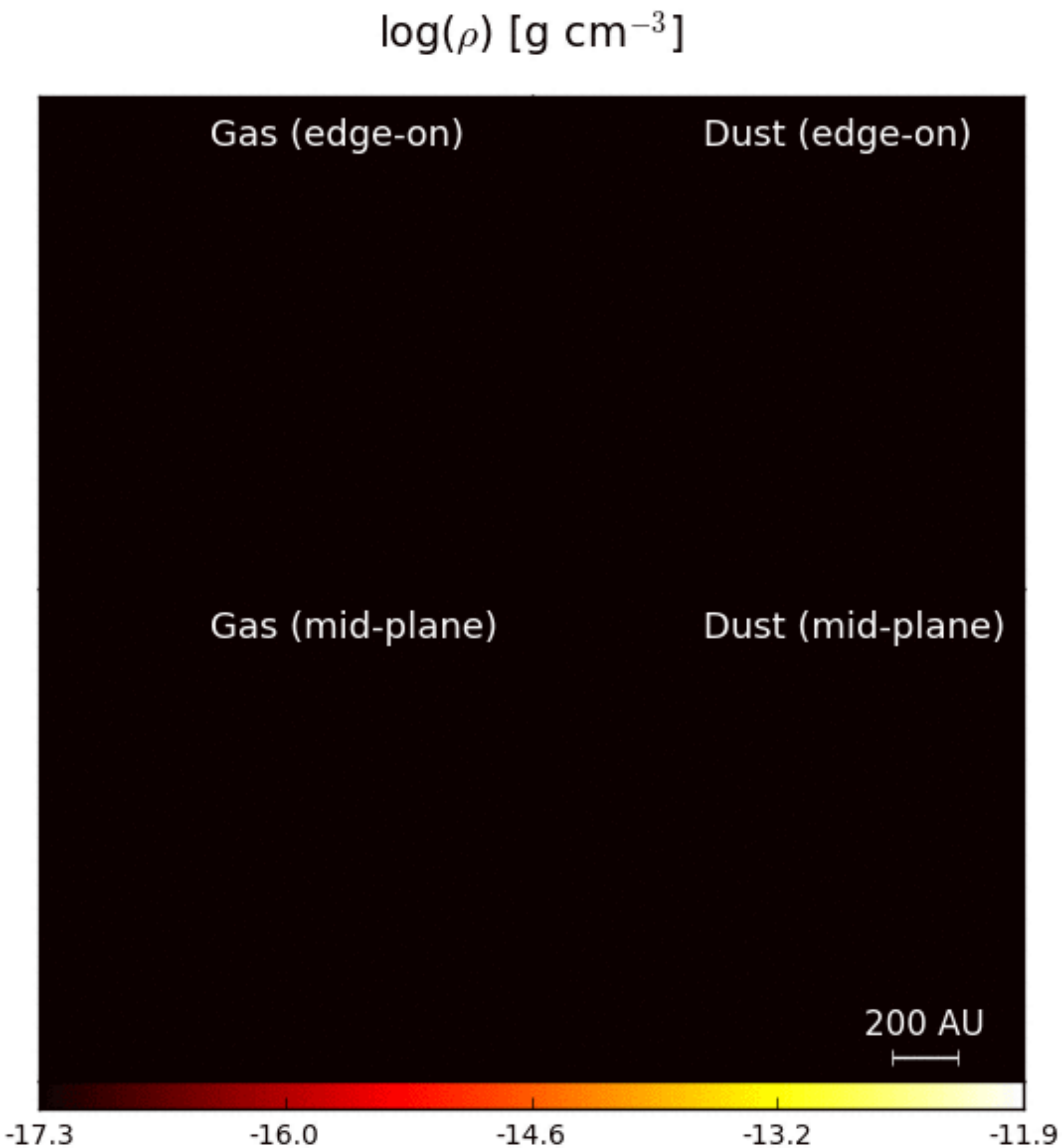

Hydro

Lebreuilly et al., 2020

Collapse with dust and gas dynamical coupling

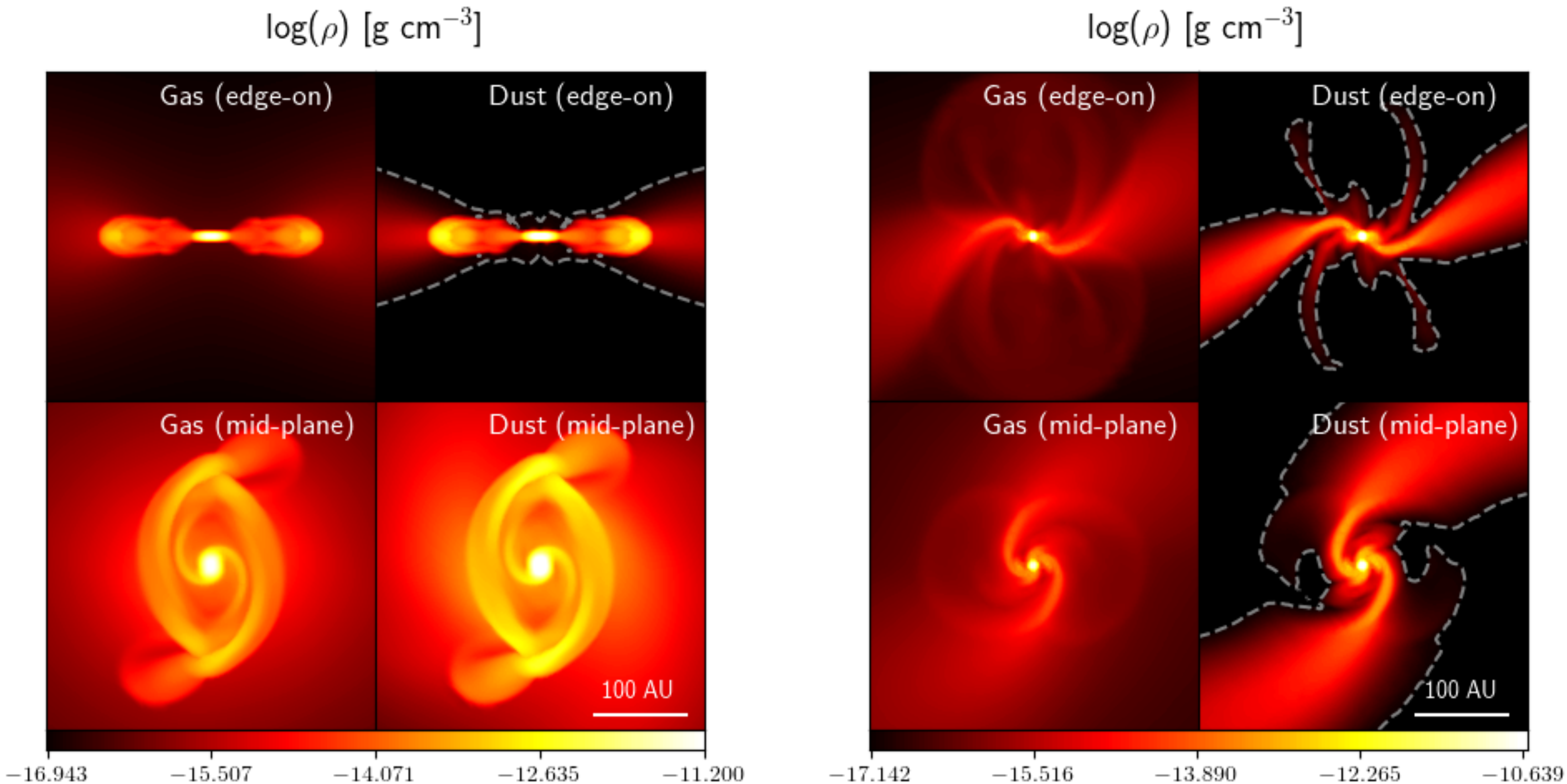

Hydro

Ideal MHD

Lebreuilly et al., 2020

Dust coagulation & MHD resistivities

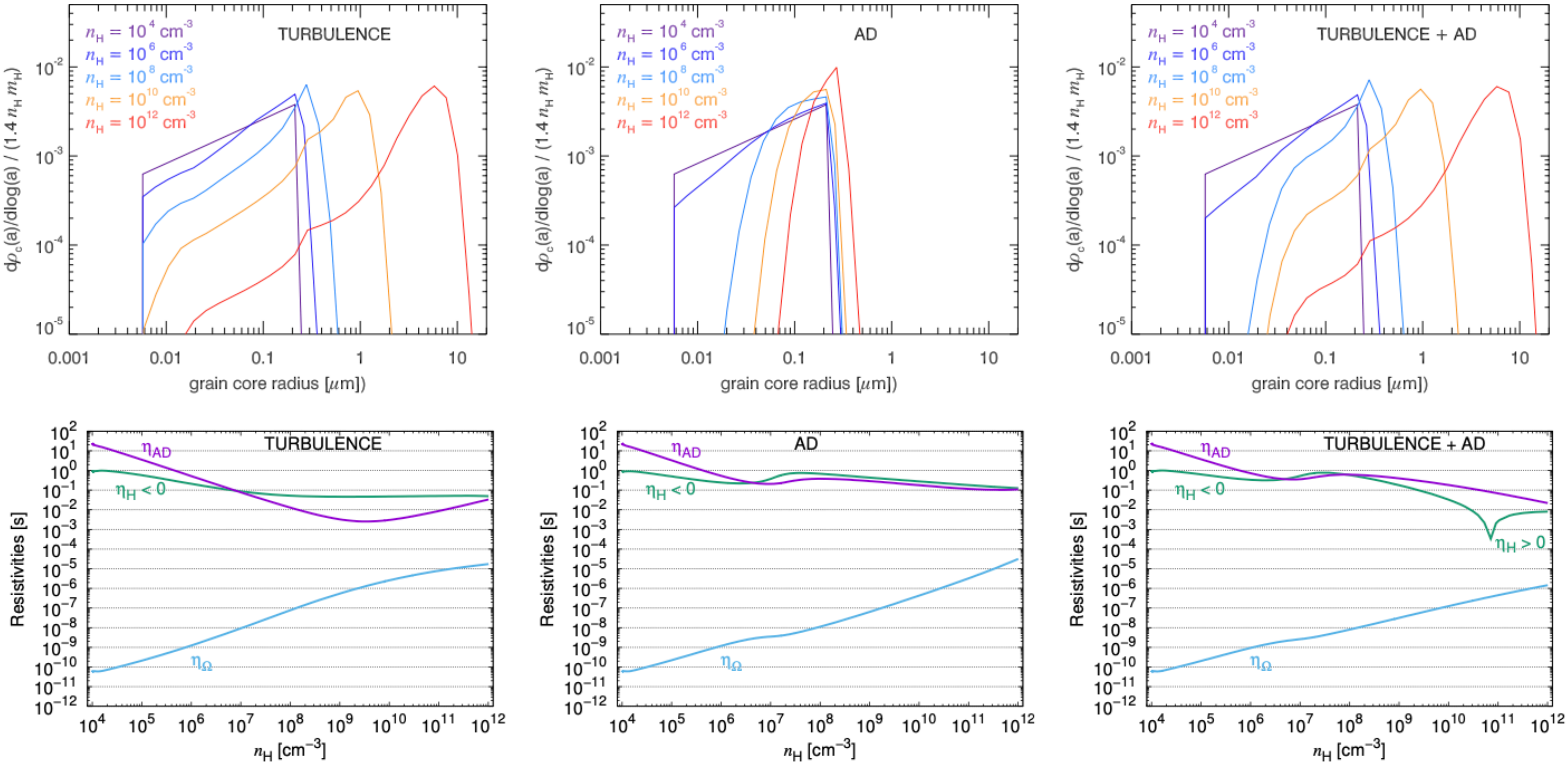

Guillet et al. (2020)

See also *Silsbee et al. (2020)*

Effect of dust grains

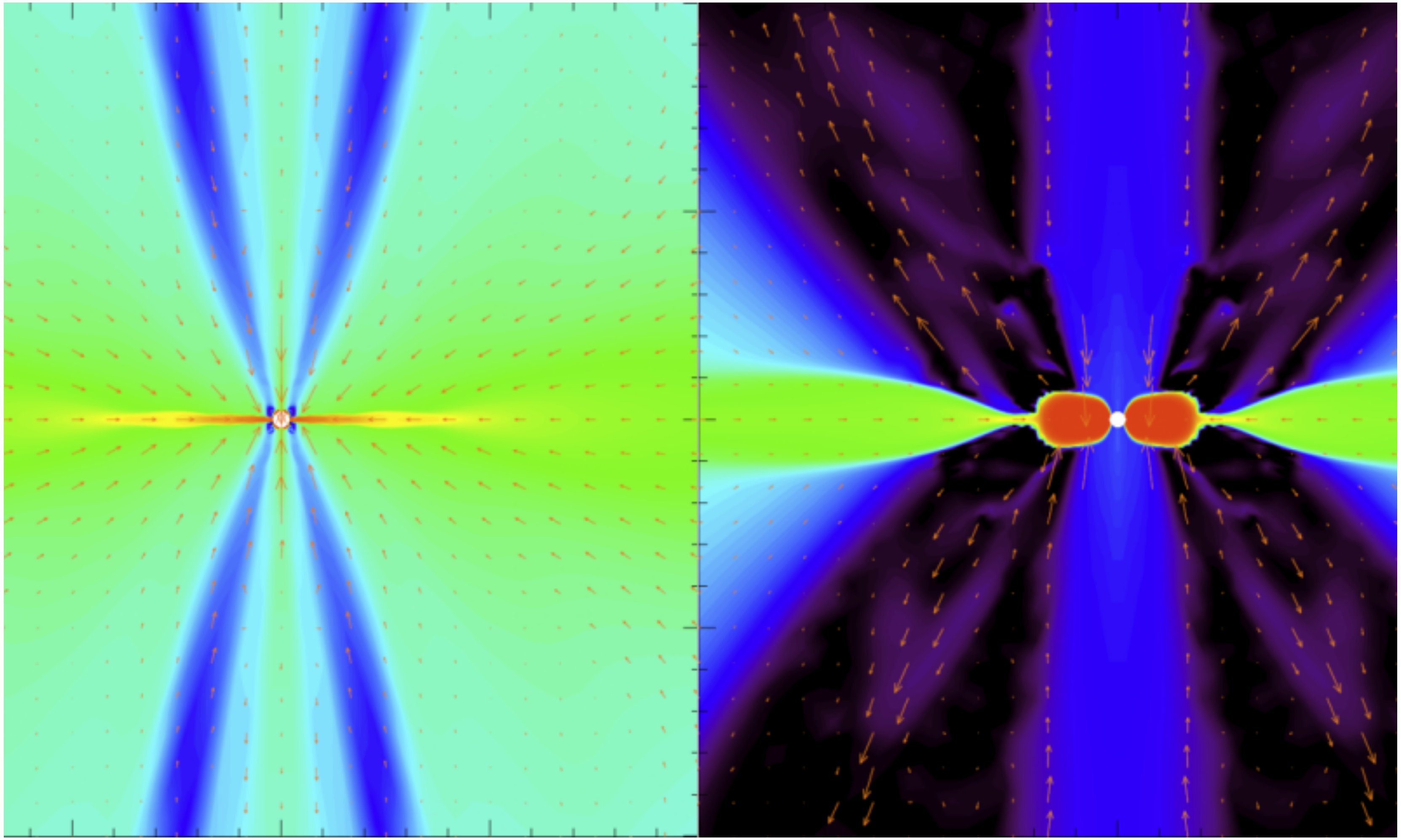

Small grains
standard MRN
amin = 0.005 μm, amax = 0.25 μm

Large grains
truncated MRN
amin = 0.1 μm, amax = 0.25 μm

Zhao et al (2016)